

Analysis of Cell Adhesion Molecules in Synapse Formation and Synaptic Transmission

Gopal Pramanik
Doctor of Philosophy

Department of Physiological Sciences, School of Life Science,
The Graduate University of Advanced Studies

2015

Acknowledgement

I express my gratitude to Prof. Katsuhiko Tabuchi for giving me an opportunity to work under his supervision. I like to thank Prof. Yumiko Yoshimura and Prof. Ryuichi Shigemoto for supervision and support for my PhD work. They helped me to develop my scientific attitude through fruitful discussions and inspiring suggestions. Under their guidance I gained the knowledge and the confidence that enabled me to compile my PhD thesis successfully. During my PhD work they were my bosses but at the same time they were my very good friends. I am very thankful to them for being available whenever I needed help.

I am deeply grateful to Prof. Jaewon Ko, Yonsei University, our enthusiastic collaborator for being a very good friend and for his excellent teaching, interaction and details regular email regarding our projects. His assistance, advices, collaborations helped me in carrying out successfully many of the experiments, and some of the experiments presented for this study were performed in his laboratory. We met in South Korea and Japan in different scientific meetings where we had the chances to discuss various projects, his support and friendliness always made our discussions both educational and enjoyable. I like to give special thanks to Prof. Katsuhiko Tabuchi for allowing me to attend several scientific meetings as well as for introducing me to his wonderful scientific friend Prof. Ko.

I am thankful to Dr. Takuya Sasaki for valuable experiences and suggestions in electrophysiology. I like to thank Dr. Daisuke Kase from the lab of Prof. Keiji Imoto for teaching me Patchmaster software, and Dr. Takeshi Uemura for teaching me molecular biology as well as artificial synapse formation assays. I like to thank all our previous and current lab members.

I am thankful to Prof. Volkmar Lessmann and Dr. Tanja Brigadski, Institute of Physiology, Germany where I learnt vesicles trafficking in neurites and part of electrophysiology experiments. My thanks also goes to Prof. Koh Cheng Gee in NTU, Singapore for supporting me to perform research in mouse and human embryonic stem cells and its differentiation to neurons.

National Institute for Physiological Sciences (NIPS), the Graduate University of Advanced Studies (Sokendai), Okazaki, Japan is one of the best brain research institutes with so many world class friendly scientists who are always accessible to guide and motivate research scholars in all circumstances. I like to thank all those scientists for their support and guidance throughout my studies. I also acknowledged support from Shinshu University School of Medicine.

I deeply indebted to German neuroscientist and my longtime friend Prof. Klaus Heese, Hanyang University, South Korea for his constant support and inspiration.

Last but not least, I like to remember supports from my parents, sisters and brother throughout my career. Thanks to my teachers and friends.

Elucidation of brain function is important for our healthy survival and understanding diseases, I like to thank all those who are guiding me in specific direction of brain research.

Respectfully yours,

<u>Contents</u>		Page
1.0.	Summary	1-4
2.0.	Introduction	5-8
2.1.	Synapse formation and synaptic transmission	6
2.2.	Cell adhesion molecules	6-7
2.3.	Calsyntenins	7
2.4.	LAR-RPTPs (Leukocyte common antigen-related receptor protein	7-8
3.0.	AIMs of the Projects	9
4.0.	Materials	10-15
4.1.	Equipment and accessories	11
4.2.	sh-RNA constructs	12
4.3.	Plasmid DNA	12
4.4.	Reagents for electrophysiology	13
4.5.	Antibodies	14
4.6.	Animals	15
5.0.	Methods	16-23
5.1.	Preparation of hippocampal neuron culture	17
5.2.	Heterologous synapse formation assays	17
5.3.	Recombinant protein preparation	18
5.4.	Cell surface binding assay	18
5.5.	Preparation of lentivirus particles	18
5.6.	Lentivirus infection of cultured hippocampal neurons	19
5.7.	In utero electroporation	19
5.8.	Slice preparation	19
5.9.	Whole cell patch clamp recording in mouse brain slice	20
5.10.	Electrophysiology in culture neurons	20
5.11.	Data acquisition and analysis	21
5.12.	Pull-down assays	21

5.13.	Affinity chromatography and in-gel digestion	22
5.14.	Mass spectrometry analysis	23
6.0	Results	24-33
Aim#1:	To address the question “How do calsyntenins regulate synapse formation and synaptic transmission?”	25
6.1.	Results -1	26-29
6.1.1.	CST-3 induces presynaptic differentiation	26
6.1.2.	Knockdown of three CSTs decreases excitatory and inhibitory synapse density in cultured mouse hippocampal neurons	26-27
6.1.3.	Knockdown of three CSTs decreases inhibitory synaptic transmission in vitro	27
6.1.4.	Knockdown of three CSTs decreases inhibitory synaptic transmission in vivo	28
6.1.5.	CST-3 interacts with Nr _x -	28
6.1.6.	CST-3 induces presynaptic differentiation through Nr _x -	28-29
Aim#2:	How do LAR-RPTPs (Leukocyte common antigen-related receptor protein tyrosine phosphatases): LAR,PTPσ, PTPδ regulate synapse formation and synaptic function?	30
6.2.	Results-2	31-33
6.2.1.	Identification of glypican-4 (GPC-4) as a potential ligand for PTP	31
6.2.2.	PTP interacts with GPC-4 through its HS-binding segment of Ig domain	31
6.2.3.	PTP interacts with cleaved GPC-4	31-32
6.2.4.	PTP induces presynaptic differentiation in concert with LRRTM4 and HS-PG	32
6.2.5.	The HS binding sequence of PTP is important for excitatory synaptic transmission in cultured rat hippocampal neurons	33

7.0.	Discussions	34-38
7.1.	Discussion-1	35-36
7.2.	Discussion-2	37-38
8.0	Figures and Legends	39-70
9.0.	References	71-76
10.0.	Abbreviations	77-82
11.0.	Curriculum Vitae	83-88
12.0.	Scientific Publications	89
13.1.	Posters	89
13.2.	Papers	89

Figure and Table index

Page

Figure 1.	Schematic representation of heterologous synapse-formation assay	40
Figure 2.	CST-3 induces presynaptic differentiation	41
Figure 3.	Quantification of the synaptogenic activities of CSTs in the heterologous synapse-formation assay	42
Figure 4.	Quantification of knockdown efficiency of CSTs shRNA lentiviruses in cultured mouse cortical neurons	43
Figure 5.	CST-TKD reduces synapse density and soma size in cultured mouse hippocampal neurons	44
Figure 6.	Effects of CST single knockdown on the synapse density and soma size in cultured mouse hippocampal neurons	45
Figure 7.	Experimental arrangement for electrophysiological recording of miniature postsynaptic currents (mEPSC/mISPC) from cultured hippocampal neurons	46
Figure 8.	CST-TKD impairs inhibitory synaptic transmission in cultured hippocampal neurons	47
Figure 9.	Procedure for in utero electroporation to introduce DNAs in the pyramidal neurons in layer 2/3 cerebral cortex	48
Figure 10.	Experimental arrangement for slice electrophysiology	49
Figure 11.	CST-TKD impairs inhibitory synaptic transmission in the pyramidal neurons in layer 2/3 cerebral cortex in mice	50
Figure 12.	Experimental arrangement for slice electrophysiological stimulation	51
Figure 13.	CST-TKD does not impair inhibitory postsynaptic paired-pulse ratio (IPSC-PPR) in layer 2/3 cerebral cortex in mice	52
Table 1.	Identification of Nr _x - as potential interaction partners for CST-3 by LC/MS/MS	53

Figure 14.	Identification of CST-3 interacting molecules	54
Figure 15.	Schematic representation of heterologous synapse-formation assay	55
Figure 16.	Nrxs are essential for CST-3-mediated presynaptic differentiation	56
Figure 17.	Quantification of the effect of Nrx triple knockdown on the synaptogenic activity of CST-3	57
Figure 18.	Schematic representation of cell surface binding assay	58
Figure 19.	CST-3 does not directly bind to Nrxs	59
Figure 20.	A proposed model for trans-synaptic interaction between presynaptic Nrxs and postsynaptic CST-3 through unidentified protein	60
Figure 21.	Identification of PTP binding partners by affinity chromatography	61
Figure 22.	Glypicans (GPCs) are heparan sulfate proteoglycans that bind to the outer surface of the plasma membrane by a glycosylphosphatidylinositol (GPI) anchor	62
Figure 23.	PTP interacts with cleaved GPC4 through immunoglobulin (Ig)	63
Figure 24.	A proposed model for LRRTM4/GPCs/PTP complex	64
Figure 25.	Schematic representation of heterologous synapse-formation assay	65
Figure 26.	PTP is required for LRRTM4-mediated presynaptic differentiation	66
Figure 27.	PTP regulates excitatory synaptic transmission through haparan sulfate interaction	67
Figure 28.	Knockdown of PTP does not change inhibitory synaptic transmission in cultured hippocampal neurons	68

Figure 29. Experimental arrangement for electrical stimulation of cultured hippocampal neurons	69
Figure 30. PTP is not essential for EPSC paired pulse ratio	70

Summary

1. Summary

Synaptic cell-adhesion molecules (CAMs) play a critical role in synapse formation and synaptic transmission. Numerous synaptic CAMs have been identified, but their physiological functions remain incompletely understood. For better understanding of the function of CAMs in synapses, I focused on two important synaptic CAM families, Calsyntenins and leukocyte common antigen-related receptor protein tyrosine phosphatases (LAR-RPTPs), and analyzed their functions in synapse formation and synaptic transmission.

Calsyntenins are postsynaptic membrane proteins consisting of cytoplasmic calcium binding domains and extracellular cadherin binding domains. Calsyntenin family comprises Calsyntenin-1, Calsyntenin-2 and Calsyntenin-3. To study the effect of Calsyntenins on synapse formation, I first employed HEK293T-neuron co-culture assay. In this experiment, I found Calsyntenin-3, but not Calsyntenin-1 and Calsyntenin-2, induced synapse formation on HEK293T cells from co-cultured rat/mouse neurons when it was overexpressed in HEK293T cells. Next I knocked down Calsyntenins in neurons and examined the effects on synapse formation and synaptic transmission. Simultaneous knockdown of Calsyntenin-1, Calsynteni-2 and Calsyntenin-3 (CST-TKD) in mouse cultured hippocampal neurons reduced synapse density both in inhibitory and excitatory synapses. CST-TKD reduced the expression of presynaptic marker synapsin-1, inhibitory presynaptic marker GAD67, excitatory presynaptic marker VGLUT1, inhibitory postsynaptic marker gephyrin, but not excitatory postsynaptic marker homer-1. However, single knockdown of any Calsyntenis did not affect synapse formation, suggesting that Calsyntenins are important for the maintenance of synapses. By using electrophysiological methods, I showed that CST-TKD in mouse cultured hippocampal neurons reduced the frequency, but not amplitude of miniature inhibitory postsynaptic currents (mIPSCs). Under my experimental conditions, the frequency and amplitude of miniature excitatory postsynaptic currents (mEPSCs) were unaltered. CST-TKD reduced the frequency but increased amplitude of mIPSCs in mouse layer 2/3 pyramidal neurons in somatosensory cortex. In contrast, CST-TKD did not alter the frequency and amplitude of mEPSCs in layer 2/3 pyramidal neurons. The paired pulse ratio (PPR) of IPSCs was unaltered in CST-TKD in layer 2/3 pyramidal neurons in somatosensory cortex. Next, I identified α -Neurexin as a binding partner for Calsyntenin-3 from rat brain extracts by using affinity chromatography, liquid chromatography and mass spectrometry. Importantly, simultaneous knockdown of

Neurexin-1, Neurexin-2, and Neurexin-3 in mouse cultured hippocampal neurons inhibited Calsyntenin-3-induced synapse formation in artificial synapse formation assay. Collectively, these results suggest that three Calsyntenins regulate synapse formation and inhibitory synaptic transmission in concert with α -Neurexin.

LAR, PTP δ and PTP σ are the members of (LAR-RPTPs) family proteins, known to be involved in synapse formation and synaptic transmission. They have common domain structures which include extracellular three immunoglobulin like domains, fibronectin type III domains, and transmembrane regions. Because extracellular domains of synaptic CAMs play an important role in their cell adhesive activity. I explored the binding protein to the extracellular domain of PTP σ . Here, I identified Glypican-4 (GPC-4) as a binding partner of PTP σ from rat brain extracts by affinity chromatography, liquid chromatography and mass spectrometry. GPC-4 is a member of vertebrate six glypicans that are heparan sulfate (HS) proteoglycans and binds to the plasma membrane through glycosylphosphatidylinositol anchor. I found that GPC-4 bound to LAR, PTP δ and PTP σ and that PTP σ interacted with only proteolytically cleaved forms of GPC-2, GPC-3, GPC-4 and GPC-6, but not full length glypicans. The interaction between PTP σ and GPC-4 depends on HS-binding because mutation of HS-binding residues (KKKK) in PTP σ to PTP σ -AAAA or (SSS) in GPC-4 to GPC-4-AAA abolished their interaction. Leucine-rich repeats transmembrane 4 (LRRTM4) induces excitatory synapse formation in artificial synapse formation assay using rat cultured hippocampal neurons, however, knockdown of PTP σ , but not LAR, inhibited this LRRTM4-induced synaptogenic activity. Wild-type PTP σ , but not PTP σ -AAAA (HS-binding deficient mutant), rescued the effect of PTP σ -knockdown on LRRTM4-induced synapse formation. Knockdown of PTP σ in rat cultured hippocampal neurons reduced both frequency and amplitude of mEPSCs. Wild-type PTP σ , but not HS-binding mutant PTP σ -AAAA reversed the effect of PTP σ knockdown on excitatory synaptic transmission. In contrast, knockdown of PTP δ in rat cultured hippocampal neurons reduced the frequency, but not amplitude of mIPSCs. Knockdown of LAR and PTP σ did not affect the frequency and amplitude of mIPSCs. In addition, knockdown of PTP σ did not affect the PPR of EPSCs. Together these results suggest that presynaptic PTP σ and GPC-4 regulate excitatory synapse formation and synaptic transmission in HS-dependent manner. Electrophysiological data suggests that PTP δ may

regulate inhibitory synaptic transmission. Further, LRRTM4 may induce excitatory synapse formation through LRRTM4, PTP σ and GPC-4 complex.

In conclusion, I showed that postsynaptic Calsyntenins redundantly regulate inhibitory synapse formation and synaptic transmission through interaction with presynaptic α -Neurexin. In addition, I found that presynaptic PTP σ forms complex with presynaptic glypican-4 and postsynaptic LRRTM4, and modulates excitatory synaptic transmission. These results should contribute to understanding the molecular mechanisms for synapse formation and synaptic transmission in mammalian brain.

Introduction

2. Introduction

2.1. Synapse formation and synaptic transmission:

Synapse is a specialized structure between two neurons, at which information required for neural activity is transferred. Sherrington coined the term "synapse" in 1879. Billions of neurons make interconnections to form trillions of synapses in human brain. Synapse is classified in two types: chemical synapse and electrical synapse. In chemical synapse, electrical activity in the presynaptic neurons is converted into the neurotransmitter release that activates receptors of postsynaptic neurons. Synapses can undergo structural and functional changes in experience dependent manner called activity dependent plasticity. These activity dependent synaptic modifications are thought to be important for memory storage. Precise synapse formation and neuronal circuit assembly during development are crucial for correct function of the brain. Disturbance in synaptic function causes several brain disorders such as autism spectrum disorders (ASDs), depression, anxiety, addiction, dementia, and insomnia. Brain diseases are major impediment in the society. Understanding of synapse in molecular levels is expected to help to cure or prevent various psychological disorders (reviewed in Lüscher et al., 2009).

2.2. Cell adhesion molecules:

Cell adhesion molecules (CAMs) are cell surface molecules responsible for cell-cell interaction or cell-matrix interaction. They are also known to be involved in the regulation of various cellular processes including cell cycle control, development, cellular communication, cell movement, synaptic transmission and synaptic plasticity. CAMs in synapses are called synaptic CAMs. The first indication of synaptic CAMs is the observation of pre- and postsynaptic processes and thick bands of extracellular molecules in synaptic cleft in electron micrograph of rat visual cortex (Gray 1959). Some specific synaptic CAMs trigger pre- and postsynaptic differentiation and mediate synaptic functions (reviewed in Missler et al, 2012). These synaptic CAMs are so-called "synapse organizers". Recently, several synapse organizers have been identified, such as neuroligins (NLs), leucine-rich repeats transmembrane (LRRTMs) and Slit- and Trk-like family proteins (Slitrks). Their adhesive and functional specificities are performed through their extracellular domains such as

immunoglobulin (Ig) domain, cadherin domain, laminin/neurexin/sex hormone-binding globulin (LNS) domain, fibronectin (FN) domain and leucine-rich repeats. However, the molecular basis of extracellular region of synaptic CAMs is not fully understood.

2.3. Calsyntenins (CSTs):

CST family is an evolutionally conserved type I transmembrane protein with extracellular region containing two cadherin repeats and LNS domain. The mammalian CST family comprises three proteins (CST-1, CST-2 and CST-3). CST-1 is expressed throughout mouse brain but is more strongly expressed in the hippocampus and the cerebral cortex. On the other hand, CST-2 and CST-3 are mainly expressed in interneurons in the mouse brain (Voigt et al., 2001; Hintsch et al., 2002). CST-1 is packaged in vesicles and is likely to be transported by kinesin-1 in calcium-dependent manner because a mutation in cytoplasmic calcium binding domain of CST-1 perturbs transportation of CST-1 containing vesicles (Konecna et al., 2006; Ludwig et al., 2009). CST-1 was reported to be associated with Alzheimer's disease (Steuble et al., 2012). CST-1 is highly up-regulated in cerebrospinal fluid in dementia with Lewy bodies patient (Dieck et al., 2013). *C.elegans* ortholog CASY-1 is essential for associative learning (Ikeda et al., 2008; Hoerndli et al., 2009). CSTs are linked to presynaptic adhesion molecule Nrxa (Pettem et al., 2013; Um et al., 2014). CST-1 was reported to regulate dendritic spine maturation and NMDA receptor targeting in mouse CA1 hippocampal pyramidal cells (Ster et al., 2014). The researches on CSTs are rapidly increased because of its emerging implications in brain function and disease.

2.4. Leukocyte common antigen-related receptor protein tyrosine phosphatases (LAR-RPTPs):

Receptor protein tyrosine phosphatases (RPTPs) play roles in many cellular processes. Based on the structures of the extracellular domains, RPTPs are classified into the eight types (type I to type VIII). LAR-RPTPs are type IIa RPTPs composed of LAR, PTP α , and PTP β in vertebrates. LAR-RPTPs have a single transmembrane region, an extracellular region consisting of three Ig-like and four FN type III (FNIII) domains, and two cytoplasmic

phosphatase domains (reviewed in Johnson et al., 2003 and Um et al., 2013). The synaptic functions of LAR-RPTPs are evolutionarily conserved. In invertebrates, LAR-RPTPs orthologs (dLAR in *Drosophila melanogaster* and HmLARs in *Hirudo medicinalis*) play important roles in synaptic development (Tian et al., 1991; Desai et al., 1994; Gershon et al., 1998). Recent studies in vertebrate have shown that mammalian LAR-RPTPs are involved in neuronal development. They play crucial roles in synapse formation and function through binding with various postsynaptic ligands (reviewed in Takahashi et al., 2013 and Um et al., 2013). Presynaptic LAR, PTP^α and PTP^β bind trans-synaptically to postsynaptic Netrin-G ligand 3 (NGL-3) (Woo et. al., 2009). PTP^α binds to TrkC (Takahashi et al., 2011). PTP^β binds to interleukin-1-receptor accessory protein like 1 (IL1RAPL1) (Yoshida et al., 2011). PTP^α and PTP^β, but not LAR, bind to Slitrks (Takahashi et al., 2012; Yim et al., 2013). These ligands exist only in vertebrates. Thus, molecular basis of extracellular region of LAR-RPTPs family is not fully understood.

3. AIMS of the Projects

3.1. Aim#1: To address the question "how do CSTs regulate synapse formation and synaptic transmission?"

3.2. Aim#2: To address the question "how do LAR-RPTPs (LAR, PTP , and PTP) regulate synapse formation and synaptic function?"

Materials

4. Materials

4.1. Equipment and Accessories:

Name	Company	specification
Double patch clamp apparatus	HEKA	EPC 10 USB
Borosilicate glass pipette for patch clamp recording	Shutter Instruments	BF150-86-10, with filament
Borosilicate Theta glass pipette for stimulation	Shutter Instruments	BT150-10
Borosilicate glass pipette for in utero electroporation	Shutter Instruments	B150-86-10, without filament
Pipette puller	Shutter Instruments	Model P-1000
Brain slicer	Campden Instruments	Ci 7000smz
Electroporator for <i>in utero</i> electroporation	NEPA Gene	CUY21
Bipolar electrode	Inter Medical Co. Ltd, Japan.	IMJ2-10H50-0.05
Microscope for patch clamp	Olympus	
Camera	Hamamatsu	C11440
Confocal microscope	Leica	
Patchmaster Software	HEKA	
Minianalysis Software	Synaptosoft	Ver 6.1

4.2. shRNA constructs:

Name	Target Sequence	
L309	Lentiviral backbone vector	
L309-sh-CST-1	5 ϕ -CTG TGG ACA AAG AC GTTATA- 3 ϕ	Um et. al., 2013
L309-sh-CST-2	5 ϕ -CGG AGT CAT AAC TGAGAACAA-3 ϕ	Um et. al., 2013
L309-sh-CST-3	5 ϕ -CCA AGG TCT TAC TGT CTC TAT-3 ϕ	Um et. al., 2013
L309-sh-PTP	5 -GCC ACA CAC CTT CTA TAA T-3	Yim et. al., 2013
L309-sh-PTP	5 -GTG CCG GCT AGA AAC TTG T-3	Yim et. al., 2013
L309-sh-LAR	5 -GCC TAC ATA GCT ACA CAG-3	Yim et. al., 2013
L315-Nrx-1	5 -GTG CCT TCC TCT ATG ACA ACT-3	Zhang et. al., 2010
L315-Nrx-2	5 -GAA CAA AGA CAA AGA GTA T-3	Zhang et. al., 2010
L315-Nrx-3	5 -ATG CTA CAC TTC AGG TGG ACA-3	Zhang et. al., 2010
LRRTM1	5 -CAG CCT CAA GTT TCT CGA CAT-3	Ko et al., 2011
LRRTM2	5 -GCT ACA ACT TAT AGA GAT CCA-3	Ko et al., 2011

4.3. Plasmid DNA:

The following plasmid constructs were obtained from Prof. Jaewon Ko, Yonsei University, South Korea, as a part of our collaborative research; pDisplay-GPC-1, pDisplay-GPC-2, pDisplay-GPC-3, pDisplay-GPC-4, pDisplay-GPC-5, pDisplay-GPC-6, pDisplay-GPC-4 AAA (mutated from SSS), p3CPro-GPC-4, p3CPro-GPC-4 351-AISA, pCMV5-LRRTM2-mVenus, pEGFP-N1 LRRTM4, pDisplay-LRRTM4, pDisplay-Slit1, pCMV5-IgC, pDisplay-HA-CST-1, pDisplay-HA-CST-2, pDisplay-HA-CST-3.

4.4. Reagents for electrophysiology:

Reagent	company	Cat.No
cesium chloride	nakarai	07806-92
cesium hydroxide monohydrate	nakarai	07828-54
EGTA	nakarai	15214-92
50 % gluconic acid	wako	078-00405
Na-GTP	sigma	G8877
Mg-ATP	sigma	A9187
strontium chloride hexahydrate	nakarai	32309-45
potassium gluconate	sigma	G4500
HEPES	sigma	H4034
CNQX	Tocris	0190
DNQX	Tocris	2312
APV	Tocris	3693
TTX	Abcam	Ab120055
QX315	Ascent	APN07066-1-1
Picrotoxin	Ascent	APN10233-1-2

4.5. Antibodies:

Name	description
JK001	rabbit anti-CST-3 antibody (peptide sequence used CSDERRIIESPPHRY)
JK010	rabbit anti-CST-2 antibody (aa 818-912)
rabbit polyclonal anti-synapsin I	Millipore
guinea pig polyclonal anti-VGLUT1	Millipore
mouse monoclonal anti-GAD67	clone 1G10.2; Millipore
mouse monoclonal anti-PSD-95	clone 7E3-1B8; Thermo Scientific
mouse monoclonal anti-HA	clone HA-7; Covance
goat polyclonal anti-EGFP	Rockland
mouse monoclonal anti-gephyrin	(clone mAb7a; Synaptic Systems)
mouse monoclonal anti-synaptophysin	clone SVP-38; Sigma
rabbit polyclonal anti-MAP2	Sigma
mouse monoclonal anti-MAP2	clone HM-2; Sigma
mouse monoclonal anti- α -tubulin	clone DM1A; Hybridoma Bank
rabbit 1133 polyclonal anti-Homer1	gift from E. Kim, KAIST, Taejon, Korea
mouse monoclonal anti-NL1	clone N97A/31; NeuroMab
rabbit polyclonal anti-LRRTM4	Abcam
mouse monoclonal anti-LRRTM4	clone N205B/22; NeuroMab
rabbit monoclonal anti-GPC-4	aa 88-101; Immundiagnostik
rabbit monoclonal TrkC	clone C44H5; Cell Signaling
mouse monoclonal anti-PTP	clone 17G7.2; MediMabs

4.6. Animals:

Time mated pregnant Wistar rats (*Rattus norvegicus*) were purchased from Japan SLC international (<http://jslc.co.jp>) and kept in laboratory animal house for 2-5 days to give birth to the pups. The pups at postnatal day zero to three (P0-P3) were used for hippocampal neuron cultures. Time mated ICR mice (*Mus musculus*) were purchased from Japan SLC international (<http://jslc.co.jp>) and kept in laboratory animal house for 2-5 days to give birth to the pups. The pups at postnatal day zero to three (P0-P3) were used for hippocampal neuron cultures. Time mated ICR mice (*Mus musculus*) at embryonic days 14.5 (E14.5) were purchased from CLEA-Japan international (<http://www.clea-japan.com>) and kept in laboratory animal house for one day and used for in utero electroporation at E15.5. Animal handling was conducted according to the guidelines of National Institute for Physiological Sciences, The Graduate University of Advanced Studies (<http://www.nips.ac.jp>), Okazaki, Japan and Shinshu University School of Medicine, Matsumoto, Japan.

Methods

5. Methods

5.1. Preparation of hippocampal neurons:

Hippocampi were removed from postnatal day 0 (P0) -P3 ICR mouse or Wistar rat pups and placed into ice-cold modified phosphate-buffered saline (mPBS) containing 1 mg/ml BSA, 6 µg/ml DNase I, 10 mM glucose, 1 mM Glutamax (Life Technologies), 1.8 mM NaOH, 56 µg/ml Phenolred, 1 mM Pyruvate (Gibco), 1 mM CaCl₂, 5.8 mM MgCl₂ and penicillin/streptomycin. Fourteen hippocampi were trypsinized with mPBS containing 0.25% trypsin (Gibco) for 10-15 min at 37 °C with gentle mixing. The cells were dissociated by passing through a 1 ml pipette (5-7 times) followed by passing through 200 µl pipette (5-7 times). Trypsin was inactivated by adding basal modified Eagle (BME; Life Technologies) medium supplemented with 10% FCS, 5 mM glucose, 10 mM Glutamax, 10 mM HEPES, 18 µg/ml insulin, and penicillin/streptomycin and centrifuged at 1,000 rpm for 10 min at room temperature. The cells were suspended in the same BME medium and plated at a density of approximately 8.5×10^4 cells/cm² on polyethylenimine (PEI)-coated glass coverslips (12 mm diameter). The glass coverslips (12 mm diameter; Matsunami Glass Ind., Ltd, Japan) were coated with 1% PEI for 3-4 hours and then washed with sterile water several times, followed by drying under laminar flow with UV light sterilization. After 8-24 hours, cultured medium was replaced with Neurobasal medium (Life Technologies) supplemented with 10 mM Glutamax, 0.025 unit/ml PEST and 2% B27-supplement (Life Technologies).

5.2. Heterologous synapse formation assay:

HEK293T cells were used for heterologous synapse formation assay as described previously (Scheiffele et al., 2000). HEK293T cells were transfected with pEGFP-N1, pCMV-5-NL1-mVenus, pDisplay-HA tagged CST-1 (HA-CST-1), -2 or -3 using 1% (w/v) PEI (Sigma) solution. After 48 hours, transfected HEK293T cells were trypsinized and added to the cultured mouse or rat hippocampal neurons at days in vitro (DIV) 8-10. The co-cultured cells were immunostained at DIV 11-14 with antibodies against EGFP or HA and synapsin 1, VGLUT1, or GAD67. Fluorescent images were taken by confocal microscope, and images were analyzed using ImageJ (NIH) and Metmorph software (Molecular devices).

5.3. Recombinant protein preparation:

HEK293T cells were transfected with pDisplay-Nrx-1-Ig or pDisplay-Nrx-1-Ig. Four days after transfection, culture media were collected and centrifuged at $1,000 \times g$ to remove particles and cell debris. The supernatants were added with 20 mM HEPES (pH 7.4), 1 mM EDTA and protease inhibitor cocktail (Thermo Scientific) and incubated with protein-A sepharose (GE Healthcare). After washing with PBS, the Ig fused proteins were eluted from protein-A sepharose with 0.1 M glycine (pH 2.5) and eluted fraction was neutralized with 1 M Tris-HCl (pH 8.0).

5.4. Cell surface binding assay:

HEK293T cells were transfected separately with pDisplay-CST-1-HA, pDisplay-CST-2-HA, pDisplay-CST-3-HA or pDisplay-NL-1-mVenus. Transfected HEK293T cells were incubated with purified soluble 0.2 μ M Ig, Ig-Nrx-1 or Ig-Nrx-1 proteins. The interactions were detected by immunostaining with anti-human Ig antibody. Fluorescent images were taken by confocal microscope.

5.5. Preparation of lentivirus particles:

HEK293T cells were transfected with L309, L313, L309-CST-TKD, L313-Nrxs-TKD, L309-sh-LAR, L309-sh-PTP, L309-sh-PTP, L309-sh-LAR-sh-PTP, L309-sh-PTP wt rescue, or L309-sh-PTP-AAAA together with RRE, pVSVG and pREV by using PEI or calcium phosphate method. After 24 hours, the transfected cells were incubated with fresh Dulbecco's Modified Eagle Medium (DMEM) containing 10% FCS for 48-72 hours. The culture media containing virus particles were collected and centrifuged at $1,0000 \times g$ overnight at 4°C . The supernatants were discarded and virus particles were suspended in PBS.

5.6. Lentivirus infection of cultured hippocampal neurons:

Hippocampal neurons were infected with lentivirus expressing shRNAs at DIV 3. Three days after infection, the neurons were infected with lentivirus expressing shRNA resistant rescue genes. Cultured neurons were used for electrophysiological recording at DIV14-16.

5.7. In utero electroporation:

Plasmids were prepared by using the Endo Free Plasmid Kit (Qiagen). Timed pregnant ICR mice were anesthetized with sodium pentobarbital (Somnopenyl, KS, Tokyo, Japan). After sterilizing the abdomen with 70% ethanol, a 2-cm midline laparotomy was performed, and the uteri were moved out. For DNA microinjection, glass capillary with tip diameter ~50 μm was used. DNA mixtures were prepared with PBS containing 3 mg/ml CST shRNA, 2 mg/ml EGFP and 0.1% fast green. 1-3 μl of DNA mixture was injected into lateral ventricle of each embryo followed by application of electric pulses. The operation was completed within 30 min and the mice were transferred on 37 $^{\circ}\text{C}$ plate until recovery. Transfected pups were selected by EGFP signals detected by blue light over the skulls.

5.8. Slice preparation:

Experiments were performed on coronal slices (350 μm thickness) from P12 to P20 ICR mice. Animals were decapitated after anesthesia by diethyl ether. The brain was quickly removed from the skull and placed in ice cold artificial cerebrospinal fluid (ACSF) containing (mM): 238 sucrose, 2.5 KCl, 1 NaH_2PO_4 , 26 NaHCO_3 , 3.3 MgSO_4 , 10 glucose, 0.5 CaCl_2 , 3 myo-inositol, 0.5 ascorbic acid, 2 Na-pyruvate, saturated with 95 % O_2 and 5 % CO_2 (pH 7.4; osmolarity:~310 mosmol/kg). The chilled brain was dissected to remove the olfactory bulb and cerebellum, and subsequently glued onto a metal platform and placed in the chamber of a vibratome (Campden 7000smz) filled with ice-cold slicing solution. Coronal sections of 350 μm thick brain slices were prepared and transferred to a chamber containing ACSF continuously saturated with 95% O_2 and 5% CO_2 for recovery at 34 $^{\circ}\text{C}$ for 30 min, followed by incubation at room temperature for 1 hour.

5.9. Whole cell patch clamp recording in mouse brain slice:

Cortical neurons (layer 2/3) were visualized by infrared differential interference contrast (IR-DIC) microscopy for patch clamp experiments. Bath solution contains (in mM) 119 NaCl, 2.5 KCl, 1 NaH₂PO₄, 26 NaHCO₃, 10 glucose, 2.5 CaCl₂, 1.3 MgSO₄ saturated with 95% O₂ and 5% CO₂ (pH 7.4; osmolarity: ~310 mosmol/kg). The pharmacological blockers 1 μM tetrodotoxin (TTX), 25 μM 2-amino-5-phosphonovaleric acid (APV), 20 μM 6-Cyano-2, 3-dihydroxy-7-nitro-quinoxaline (CNQX) were used in bath solution to record mIPSCs and 1 μM TTX, 25 μM APV and 10 μM picrotoxin were used to record mEPSCs. Recording pipettes (4-6 M Ω) were filled with intracellular solution (mM): 120 cesium-D-gluconate, 10 CsCl, 5 NaCl, 10 HEPES, 10 EGTA, 4 Mg-ATP and 0.3 Na-GTP (pH 7.2; osmolarity: ~300 mosmol/kg). For recording mEPSC and mIPSCs, cesium-D-gluconate is replaced with equal amount of CsCl. To monitor the membrane statistics in each experiment, three 1 min traces were collected with a -2 mV voltage step between each trace. Theta (θ) glass capillary electrode filled with ACSF was used during stimulation to record the evoked responses. Paired-pulse facilitation experiments were performed at a holding potential of -70 mV with 100 ms inter-stimulus intervals (ISI). The amplitude of the second IPSC was measured relative to the amplitude of the first IPSC. For all whole-cell recordings, the membrane statistics were monitored after each trace. All recordings were performed with ACSF continuously saturated with 95% O₂ and 5% CO₂ at 28-30 °C. The following whole cell recording criteria were used: Ra was < 25 M Ω and cells were rejected if Ra or Rm changed 20% over the course of the experiment. All recordings were digitized at 10 kHz and filtered at 2 kHz. Recordings were monitored with EPC10 double USB (HEKA), Patchmaster software and analyzed offline using Mini Analysis Program (Synaptosoft).

5.10. Electrophysiology in culture neurons:

Cell culture electrophysiology recordings were performed using DIV 14-16 rat hippocampal cultured neurons. For whole-cell voltage clamp recordings, patch pipettes (4-7 M Ω) were filled with the following internal solution (in mM): 90 Cs-gluconate, 10 CsCl, 10 HEPES, 10 EGTA, 5 NaCl, 4 Mg-ATP, and 0.3 Na-GTP, (pH 7.2). The recordings were performed in extracellular solutions with following composition: 100 mM NaCl, 4 mM KCl, 1 mM NaH₂PO₄, 20 mM

HEPES, glycine 10 μ M, 10 mM glucose, 2 mM CaCl₂, and 1 mM MgCl₂, (pH 7.4). mEPSCs were recorded at a holding potential of -70 mV in the presence of 1 μ M TTX (Abcam), 100 μ M picrotoxin, and 50 μ M APV. For paired-pulse recordings, the concentration of CaCl₂ in the extracellular solution was increased to 4 mM, and QX314 was added to the solution to a concentration of 5 mM; recording was performed in the presence of 100 μ M picrotoxin. Bipolar electrode (Inter Medical) was placed at 100 μ m from the soma of the patched neurons and stimulated with 20, 50, 100, 150 or 200 ms inter-stimulus intervals. The amplitude of the second EPSC was measured relative to the amplitude of the first EPSC. For all whole-cell recordings, the membrane statistics were monitored after each trace by application of -2 mV, 30 ms voltage step. The following whole-cell recording criteria were used: Ra was < 25 M Ω and cells were rejected if Ra or Rm changed 20% over the course of the experiment. All recordings were digitized at 10 kHz and filtered at 2 kHz. Recordings were monitored with EPC10 double USB (HEKA) and analyzed offline using Mini Analysis Program (Synaptosoft).

5.11. Data acquisition and analysis:

Whole cell recording was performed using an EPC10 amplifier (HEKA, Germany) and acquired with Patchmaster software (HEKA, Germany). Data were filtered at 2 kHz and digitized at 10 kHz. Data analysis was performed using Minianalysis software (Synaptosoft, USA). Miniature EPSCs and miniature IPSCs were recorded in voltage clamp mode at holding potential of -70 mV. The neurons with a high seal resistance ($1 \text{ G}\Omega$) and a series resistance < 25 M Ω were selected for analysis. Data were expressed as mean \pm SEM and tested by Mann-Whitney U test or KS test (significance level $p < 0.05$).

5.12. Pull-down assays:

HEK293T cells were transfected with pDisplay-PTP, pDisplay-LAR, pDisplay-PTP, pEGFP-N1 LRRTM4, pCMV5-LRRTM3-mVenus, pCMV5-NL1-mVenus, pDisplay-GPC-1, pDisplay-GPC-2, pDisplay-GPC-3, pDisplay-GPC-4, pDisplay-GPC-4 AAA, pDisplay-GPC-5, pDisplay-GPC-6 or pDisplay-TrkC. Transfected cells were lysed and incubated with 10 μ g of Ig-PTP, Ig-GPC-4 or IgC (control) at 4 $^{\circ}$ C for 2 hours. For *in vivo* pull-down assays, rat

brain synaptosomal fractions prepared from adult (P7 and P42) rats were mixed with 10 μ g of Ig-PTP or IgC (control), and incubated at 4 °C for 4 hours. The antibodies used for immunoblotting were anti-HA (1:1000), anti-EGFP (1 μ g/ml), anti-GPC-4 (1:1000), anti-NL1 (1 μ g/ml).

5.13. Affinity chromatography and in-gel digestion:

Ten frozen rat brains were homogenized with 668 strokes with 20 ml of homogenizing buffer [320 mM sucrose, 10 mM HEPES (pH 7.4), 1 mM PMSF and a protein inhibitor cocktail], extracted with lysis buffer [50 mM Tris-HCl (pH 8.0), 150 mM NaCl, 0.1% sodium dodecyl sulfate (SDS), 0.5% Na-deoxycholate, 1 mM PMSF, protein inhibitor cocktail and 1% NP-40] and centrifuged at 100,000 \times g for 1 hour at 4 °C to pellet the insoluble materials. Protein A-Sepharose beads (GE Healthcare) bound to 100 μ g of Ig-CST-3, Ig-PTP, IgC (control) were equilibrated with lysis buffer, incubated overnight at 4 °C with 2 mg of brain extracts, centrifuged (800 \times g for 5 minutes), and washed five times with lysis buffer. The bead-bound proteins were eluted with SDS sample buffer [62.5 mM Tris-HCl, pH 6.8, 2% glycerol, 0.005% bromphenol blue, and 100 mM DL-dithiothreitol]. The eluted proteins were digested with sequencing-grade modified trypsin (Promega) and subjected to mass spectrometry. The bands that were uniquely observed in the Ig-CST-3 lane or Ig-PTP lane were directly cut from the gels, destained with 50% acetonitrile (ACN) in 50 mM ammonium bicarbonate (ABC), and dried in a speed vacuum concentrator. The gel pieces were reduced with 5 mg/ml of dithiothreitol (DTT) in 50 mM ABC at 60 °C for 1 hour, alkylated with 10 mg/ml of iodoacetamide in 50 mM ABC at room temperature for 1 hour, and dried in a speed vacuum concentrator. The dried gel pieces were rehydrated with 50 mM ABC containing 100 μ g/ml trypsin and incubated at 37°C for 16 hours. The supernatant peptide mixtures were extracted with 50% ABC in 5% formic acid (FA) for 30 minutes and dried in a speed vacuum concentrator for mass spectrometry.

5.14. Mass spectrometry analysis:

In brief, the tryptic-dried samples were analyzed using an Agilent HPLC-Chip/TOF MS system equipped with an Agilent 1260 nano-LC system, HPLC Chip-cube MS interface, and 6530 QTOF single quadrupole-TOF mass spectrometer. The dried peptide samples were re-suspended in 2% ACN/0.1% FA and concentrated on a Large-capacity HPLC Chip (Agilent Technologies). The HPLC chip was incorporated into an enrichment column (9 mm; 75 μ m I.D.; 160 nl) and then a reverse-phase column (15 cm; 75 μ m I.D.; packed with Zorbax 300SB-C18 5 μ m resin). Peptide separation was performed using a 70-minute gradient of 3-45% buffer A (0.1% FA) containing 3-45 % buffer B (90% ACN/0.1% FA) at a flow rate of 300 nl/minute. The MS and MS/MS data were acquired in the positive ion mode and the data were stored in the centroid mode. The chip spray voltage was set at 2100 V, and carried with chip conditions. The drying gas temperature was set at 325 °C with a flow rate of 3.5 L/minute. A medium isolation (4 m/z) window was used for precursor isolation. A collision energy with a slope of 3.7 V/100 Da and an offset of 2.5 V was used for fragmentation. The MS data were acquired over a mass range of 300-3000 m/z, whereas the MS/MS data were acquired over a mass range of 50-2500 m/z. Reference mass correction was activated using a reference mass of 922. Precursors were set in an exclusion list for 30 seconds after the two MS/MS spectra were acquired.

Results

Aim#1: To address the question of how do CSTs regulate synapse formation and synaptic transmission?

6.1. Results -1

6.1.1. CST-3 induces presynaptic differentiation:

In order to investigate a role of CSTs in synapse formation, I performed heterologous synapse-formation assay (Figure 1; Scheiffele et al., 2002). HEK293T cells were transfected with an expression vector for EGFP alone (negative control) or together with that for N-terminal HA-tagged CST-1 (HA-CST), HA-CST-2, HA-CST-3 or mVenus-fused NL2 (NL2-mVenus) (positive control). Transfected HEK293T cells were co-cultured with cultured rat hippocampal neurons. Four days after co-culture, the cells were fixed and immunostained with antibodies against presynaptic marker Synapsin 1, glutamatergic presynaptic marker vesicular glutamate transporter 1 (VGLUT1) and GABAergic presynaptic marker glutamic acid decarboxylase (GAD) 67. I detected accumulation of staining signals for Synapsin 1, VGLUT1 and GAD67 on the surface of HEK293T cells expressing HA-CST-3 or NL2-mVenus (Figure 2 and 3). Accumulation of Synapsin 1, VGLUT1 and GAD67 signals was hardly detectable on the surface of HEK293T cells expressing HA-CST-1 or HA-CST-2 (Figure 2 and 3). These results suggest that CST-3, but not CST-1 and CST-2, induces presynaptic differentiation.

6.1.2. Knockdown of three CSTs decreases excitatory and inhibitory synapse density in cultured mouse hippocampal neurons:

In collaboration with Prof. Jaewon Ko, Yonsei University, South Korea, I constructed a series of knockdown lentiviral vectors expressing shRNA against CSTs (Figure 4). I infected cultured mouse hippocampal neurons with these lentiviruses at DIV3. After 9-10 days, I examined knockdown efficacy of these shRNAs by using quantitative real-time RT-PCR. The CST-1, CST-2 and CST-3 shRNA suppressed the endogenous mRNA expression to ~10 %, ~20 %, and ~15 %, respectively (Figure 4).

To investigate whether CSTs are required for the maintenance of synapse structures, I infected cultured mouse hippocampal neurons with lentiviruses expressing CST-1, CST-2 and CST-3 shRNAs at DIV3. After 11 days, neurons were fixed and immunostained with antibodies against pre- and postsynaptic proteins (Figure 5A). Triple knockdown of CST-1, CST -2 and

CST-3 (CST-TKD) in cultured mouse hippocampal neurons significantly reduced the number of Synapsin 1, GAD67, VGLUT1, inhibitory postsynaptic marker gephyrin, but not excitatory postsynaptic marker Homer-1 (Figure 5B). These results suggest that CSTs regulate inhibitory and excitatory synapse formation in cultured mouse hippocampal neurons. CST-TKD also reduced soma size in MAP2 positive neurons, suggesting that CSTs affect neuronal development (Figure 5C).

Next I examined whether three CSTs are functionally redundant for the maintenance of synaptic structure. The cultured mouse hippocampal neurons were infected with lentivirus expressing CST-1, CST-2 or CST-3 shRNA at DIV3. After 11 days, neurons were fixed and immunostained with antibodies against Synapsin 1 and MAP2. However, the densities of Synapsin 1 and soma size of neurons were comparable among all groups (Figure 6B and C), suggesting that CSTs are functionally redundant. To confirm the functional redundancy of CSTs, CST-TKD neurons were infected with lentivirus expressing shRNA resistant CST-1 or CST-2 at DIV7. The effect on synapse density in CST-TKD was rescued by overexpression of CST-1 or CST-3 (Figure 6B). The reduction of soma size in CST-TKD neurons was rescued by overexpression of CST-1 and CST-3, but not by single CST-1 or CST-3 (figure 6C).

6.1.3. Knockdown of three CSTs decreases inhibitory synaptic transmission *in vitro*:

I infected cultured mouse hippocampal neurons with lentivirus expressing CST-TKD at DIV 3 and recorded mEPSC/mIPSC from pyramidal neurons at DIV 14-16 (Figure 7). The CST-TKD neurons were impaired in the frequency of inhibitory postsynaptic currents (mIPSCs) but not in excitatory postsynaptic currents (mEPSCs), suggesting that CSTs are involved in the inhibitory synapse formation and synaptic transmission (Figure 8). These results are consistent with my morphological findings of reduction of the inhibitory synapse density in the cultured mouse hippocampal neurons (Figure 6 and 7).

6.1.4. Knockdown of three CSTs decreases inhibitory synaptic transmission *in vivo*:

To confirm my *in vitro* finding, I performed *in utero* electroporation in mouse embryos at E15.5 to introduce CST-TKD together with fluorescent proteins (Ds-red or EGFP) in the pyramidal neurons in layer 2/3 somatosensory cortex (Figure 9). I prepared acute brain slices from somatosensory cortex of transgene expressing mice (P12-20) for electrophysiological recordings (Figure 10). CST-TKD reduced mIPSC frequency and increased amplitude without altering frequency and amplitudes of mEPSC (Figure 11). I placed bipolar theta glass stimulation electrode on layer 4 neurons and measured paired-pulse ratio (PPR) of IPSCs in CST-TKD neurons (Figure 12), but I did not detect significant change, suggesting that CSTs have no effect on presynaptic neurotransmitters release probability (Figure 13).

6.1.5. CST-3 interacts with Nr α :

To explore potential extracellular interacting partners for CST-3, I performed affinity chromatography using CST-3 fused immunoglobulin (Ig-CST-3) (Figure 14A and B) in collaboration with Prof. Jaewon Ko, Yonsei University, South Korea. Purified Ig-CST-3 and IgC were immobilized on protein A-Sepharose beads. The mouse brain extracts were loaded onto the affinity columns. Columns were extensively washed and the bound proteins were analyzed by SDS-PAGE (Figure 14B). The bound proteins visualized with silver staining were digested with trypsin, subjected to liquid chromatography-tandem mass spectrometry (LC/MS/MS), and identified Nr α -1, Nr α -2 and Nr α -3, as potential CST-3-interacting molecules (Figure 14; Table 1).

6.1.6. CST-3 induces presynaptic differentiation through Nr α :

I examined whether Nr α s were essential proteins for CST-3-mediated presynaptic differentiation. The cultured mouse hippocampal neurons were infected with lentivirus expressing Nr α triple knockdown shRNA (Nr α -TKD). The Nr α -TKD neurons were co-cultured with HEK293T cells expressing HA-CST-3, HA-NL-1 (positive control; Gokce et. al., 2013) or HA-Slitrk-1 (negative control; Yim et. al., 2013). The accumulation of Synapsin 1 signal on HEK293T cells expressing HA-CST-3 was significantly reduced in Nr α -TKD

neurons (Figure 16 and 17). On the other hand, accumulations of Synapsin 1 signal on HEK293T cells expressing HA-Slitrk-1 were comparable between control shRNA and Nrxt-KD neurons (Figure 16 and 17). These results suggest that CST-3 induces presynaptic differentiation through the interaction with Nrxt- .

6.1.7. CST-3 does not directly interact with Nrxt- :

I showed that Nrxt- were functional receptors for CST-3 (Figure 16 and 17). Next, I examined whether Nrxts interact directly with CSTs. To address this question, I examined direct binding between CST-3 and Nrxts using cell-surface binding assay. HEK293T cells were transfected with HA-NL1, HA-CST-1, HA-CST-2 or HA-CST-3. The transfected cells were incubated with purified Ig fused Nrxt-1 (IgNrxt-1 -1) or Ig fused Nrxt-1 (IgNrxt-1 -1), followed by immunostaining with fluorescent labeled anti-Ig antibody (Figure 18). I detected strong Ig signals on the surface of HEK293T cells expressing HA-NL1. However, Ig signals were hardly detectable on the surface of HEK293T cells expressing CST-1, CST-2, and CST-3 (Figure 19). These results suggest that CST-3 does not directly bind to Nrxts.

Aim#2: To address the question of how do Leukocyte common antigen-related receptor protein tyrosine phosphatases (LAR-RPTPs): LAR, PTP α , and PTP β regulate synapse formation and synaptic function?

6.2. Results-2

6.2.1. Identification of glypican-4 (GPC-4) as a potential ligand for PTP σ :

In collaboration with Prof. Jaewon Ko, Yonsei University, South Korea I identified novel ligands for PTP σ by affinity chromatography using recombinant extracellular domain of PTP σ and immunoglobulin fusion protein (Ig-PTP σ) (Figure 21A). I incubated immobilized IgC (control) and Ig-PTP σ with rat brain synaptosome extracts. After extensive washing, bound proteins were analyzed by SDS-PAGE and silver staining (Figure 21B). The protein bands were digested with trypsin, subjected to LC/MS/MS (Figure 21G for brief flow chart of the experiments), and analyzed using Mascot software. Among identified peptides, three were derived from GPC-4. GPC-4 is a membrane glycosylphosphatidylinositol (GPI) anchor heparan sulfate proteoglycan (HS-PG) (Figure 22) which plays important roles in modulating developmental signaling pathways including fibroblast growth factor (FGF), Hedgehog, and Wnt signaling pathways (reviewed in Lin X, 2004). Previously, GPC-2 was shown to interact with PTP σ to promote outgrowth of dorsal root ganglion neurons (Coles et al., 2011). However, there is no evidence for the direct interaction of PTP σ with other GPCs.

6.2.2. PTP σ interacts with GPC-4 through its HS-binding segment of Ig domain:

To examine the direct interaction between PTP σ and GPC-4, I performed pull down assays using purified Ig-GPC-4 and HEK293T cell lysates expressing HA-tagged PTP σ (HA-PTP σ), HA-PTP σ -AAAA (HS binding-deficient mutant of PTP σ in which four lysines of the first Ig domain were replaced with alanines), HA-tagged LAR (HA-LAR), HA-tagged PTP σ (HA-PTP σ), and NL1-mVenus. I found that Ig-GPC-4 interacted with HA-PTP σ , HA-LAR and HA-PTP σ , but not with NL1-mVenus (Figure 23A). These results suggest that PTP σ , LAR and PTP σ bind to GPC-4. In addition, HA-PTP σ -AAAA abolished the interaction with GPC-4, suggesting that PTP σ requires HS for interaction with GPC-4.

6.2.3. PTP σ interacts with cleaved GPC-4:

To further examine the interaction between PTP σ and GPC-4, I performed pull down assays using Ig-PTP σ and HEK293T cell lysates expressing HA-tagged GPC-1 (HA-GPC-1), HA-

GPC-2, HA-GPC-3, HA-GPC-4, HA-GPC-5, and HA-GPC-6. I found that Ig-PTP specifically bound to cleaved GPC-2, GPC-3, GPC-4 and GPC-6, but not to uncleaved GPCs. No band was detectable from HEK293T cells transfected with an expression vectors for HA-GPC-1 and HA-GPC-5 (figure 23B), suggesting that GPC-1 and GPC-5 are not efficiently processed in these cells. In addition, HS binding-deficient mutant of GPC-4 (GPC-4-AAA) in which the HS-binding sites (Ser449, Ser495 and Ser500) were replaced with alanines abolished the interaction with Ig-PTP (Figure 23B). These results suggest that PTP interacts with cleaved GPC-4 through the HS-binding.

6.2.4. PTP σ induces presynaptic differentiation in concert with LRRTM4 and HS-PG:

LRRTM4 regulates excitatory synapse formation through a trans-synaptic interaction with GPC-4. The interaction between HS and GPC-4 is essential for the interaction of GPC-4 with LRRTM4 (de Wit J et al., 2013; Siddiqui TJ et al., 2013). Furthermore, GPC-4 is GPI anchor protein (Lin X 2004), and it needs other co-receptor/receptors for intracellular signaling. Based on the result of the direct interactions of GPCs with LAR-RPTPs (Figure 23) and the previous observations, I hypothesized that PTP σ might be a functional receptor for LRRTM4 (see proposed model in Figure 24).

To address this hypothesis, I examined whether LRRTM4 requires LAR-RPTPs for its synaptogenic activity. The cultured rat hippocampal neurons were infected with lentivirus expressing sh-LAR or sh-PTP σ , and co-cultured with HEK293T cells expressing LRRTM2 or LRRTM4. The co-cultured cells were fixed and immunostained with antibody against Synapsin 1 (figure 26A). The accumulation of Synapsin 1 signal on HEK293T cells expressing LRRTM4 was significantly reduced in LAR and PTP σ knockdown neurons (Figure 26A and B). On the other hand, accumulations of Synapsin 1 signal on HEK293T cells expressing LRRTM2 were comparable among three groups (sh-control, sh-LAR, and sh-PTP σ) (Figure 26A and B). In addition, wild-type PTP σ , but not PTP σ -AAAA, rescued the synaptogenic activity of LRRTM4 in PTP σ -knockdown cultured rat hippocampal neurons. These results suggest that PTP σ requires for LRRTM4-mediated presynaptic differentiation.

6.2.5. The HS binding sequence of PTP σ is important for excitatory synaptic transmission in cultured rat hippocampal neurons:

Finally, I examined whether the HS-binding of PTP σ is involved in synaptic functions. I infected cultured rat hippocampal neurons with lentiviruses expressing control shRNA, sh-LAR, sh-PTP, or sh-LAR/sh-PTP. Knockdown of PTP σ , but not LAR, reduced both frequency and amplitude of mEPSCs in cultured rat hippocampal neurons (Figure 27). Simultaneous knockdown of PTP σ and LAR in cultured rat hippocampal neurons also showed a significant reduction in mEPSC frequency and amplitude (Figure 27). This reduction in mEPSC frequency and amplitude in PTP σ and LAR knockdown neurons was reversed by the expression of wild-type PTP σ . Although PTP σ -AAAA rescued mEPSC amplitude, it failed to recover the mEPSC frequency (Figure 27). Knockdown of PTP σ and LAR did not affect the PPR of EPSCs. Next, I examined the roles of LAR-RPTPs in inhibitory synaptic functions. Knockdown of LAR and PTP σ did not affect the frequency and amplitude of mIPSCs (Figure 28). In contrast, knockdown of PTP δ in cultured rat hippocampal neurons reduced the frequency, but not amplitude of mIPSCs (Figure 28). I examined the EPSC paired pulse ratio (PPR) in cultured rat hippocampal neurons (Figure 30 for experimental arrangements) at 20, 50, 100, 150 and 200 ms inter stimulus interval (ISI) in control shRNA or sh-LAR/sh-PTP infected neurons (Figure 30). There was no detectable change between control shRNA and sh-LAR/sh-PTP infected neurons (Figure 30). My results collectively suggest that presynaptic PTP σ , together with GPC-4, acts in a HS-dependent manner to maintain excitatory synapse development and function.

Discussion

7.1. Discussion-1

I identified that Nr_x- was a functional interacting partner for CST-3. I showed that CST-3, but not CST-1 and CST-2, induced presynaptic differentiation in heterologous synapse-formation assay. CST-TKD reduced both inhibitory and excitatory synapse density in cultured mouse hippocampal neurons. It also reduced inhibitory synaptic transmission in *in vitro* and *in vivo*. Furthermore, all three CSTs knockdown reduced the soma size in cultured mouse hippocampal neurons. These results suggest that CSTs are important for synaptic structure, function and neuronal development.

By heterologous synapse-formation assay, I showed that CST-3 induced presynaptic differentiation whereas CST-1 and CST-2 did not (Figure 2 and 3). These results are consistent with analyses from Pettem et al., (2013).

CST-3 is a receptor for Nr_x- , but not for Nr_x- (Figure 14; Pettem et al., 2013; Lu et al., 2014). On the other hand, both Nr_x- and Nr_x- bind to NLs and LRRTMs (Boucard et al., 2005; Siddique et al., 2010). Knockdown of all three CSTs in cultured mouse hippocampal neurons reduced the densities of inhibitory and excitatory synapses (Figure 5 and 6). On the other hand, the CST-TKD reduced only the frequency of mIPSCs in *in vitro* and *in vivo* (Figure 8 and 11). CST-3 knock out (KO) in mouse impairs both inhibitory and excitatory synaptic transmission (Pettem et al., 2013). Consistent with these findings, NL triple knockdown reduces mIPSC frequency in the cultured mouse hippocampal neurons (Chih et al., 2005). These results suggest that CST-3 is a major postsynaptic organizer in inhibitory synapses through interaction with Nr_x- .

Triple knockdown of all three Nr_xs in the cultured mouse hippocampal neurons reduced CST-mediated presynaptic differentiation (Figure 16 and 17). However, the direct interaction of CST-3 with Nr_xs was not detected in my experiments (Figure 19), suggesting that CST-3 forms complex with Nr_xs through unknown proteins and induces presynaptic differentiation (Figure 20).

Aberrant CST expression has been reported in brain disorders. For example, CST-1 is highly up-regulated in cerebrospinal fluid of dementia with Lewy bodies patients (Dieck et al., 2013). CST-1 and CST-3 are up-regulated in cerebrospinal fluid of Alzheimer disease patients (Ringman et al., 2012 and Yin et al., 2009). CST-1 mediates amyloid- precursor protein

anterograde axonal transport and regulates amyloid- production (Steuble et al., 2012; Vagnoni et al., 2012). The proteolytically processed C-terminal fragment of CST-3 accumulates in dystrophic neurites surrounding amyloid- plaques in tg2576 mouse (Alzheimer disease model mice) and Alzheimer disease brains, accelerating neuronal cell death (Uchida et al., 2013). CST orthologue CASY-1 is essential for associative learning in *Caenorhabditis elegans* (Ikeda et al., 2008; Hoerndli et al., 2009; Ohno et al., 2014). Therefore, abnormal expression and regulation of CST family proteins may cause these diseases and create memory dysfunction.

In future, it is important to investigate intermediates in CST-3 and Nrxs functional complexes. Identification of other extracellular interacting partners for CST family proteins and their downstream targets are important for better understanding of their function in the brain.

7.2. Discussion-2

I identified that GPC-4 was a binding partner for PTP σ . I found that LRRTM4, GPC-4 and PTP σ formed functional complex by using heterologous synapse formation assay and this complex played important roles in synapse formation and synaptic transmission in excitatory synapses. I also showed that the HS binding residues in GPC-4 and PTP σ were important for interaction as well as for synapse formation and synaptic transmission.

LAR-RPTPs family proteins play important roles in synapse formation and synaptic transmission (reviewed in Um JW et al., 2013; Takahashi et al, 2013). Presynaptic LAR, PTP σ and PTP δ bind trans-synaptically to postsynaptic Netrin-G ligand 3 (NGL-3; Woo et al., 2009). PTP δ binds to TrkC (Takahashi et al., 2011). PTP δ binds to IL1RAPL1 (Yoshida et al., 2011). PTP δ and PTP δ bind to Slitrks (Takahashi et al., 2012; Yim et al., 2013). In the brain there are huge numbers of synapses and various cell adhesion proteins play an important role in specification and refinement of synaptic transmission resulting in precise information transfer in the brain (reviewed in Brose N, 2013). Although ligands for LAR-RPTPs family proteins have been discovered, I still believe that there are many unidentified ligands for LAR-RPTPs family proteins.

In this study, I identified GPCs as the functional ligands for PTP σ (Figure 21). I showed that PTP σ interacted with cleaved forms of GPC-2, GPC-3, GPC-4 and GPC-6, but not with uncleaved full-length GPCs. In addition, the HS binding residues of PTP σ and GPC-4 was important for the interaction between PTP σ and GPC-4 (Figure 23). Knockdown of PTP σ significantly reduced the synaptogenic activity of LRRTM4. The wild-type PTP σ , but not PTP σ -AAAA, rescued the synaptogenic activity of LRRTM4 in PTP σ -knockdown cultured rat hippocampal neurons (figure 26). I also showed that knockdown of PTP σ in the cultured rat hippocampal neurons reduced both frequency and amplitude of mEPSCs (Figure 27). Based on these results, I proposed a model for the tran-synaptic interaction of presynaptic PTP σ with postsynaptic LRRTM4 through GPCs which is essential for excitatory synapse formation and function (Figure 24).

HS-PGs are expressed in both developing (Herndon et al., 1990; Maeda et al., 2011) and adult brains (Litwack et al., 1994). Cerebroglycan, another HS-PG, is expressed specifically during neuronal differentiation (Stipp et. al., 1994). Secreted GPC-4 and GPC-6 from astrocyte

regulate AMPA receptor trafficking and consequently modulate excitatory synapse formation (Allen et al., 2012). It is also possible that PTP /GPC-4/LRRTM4 complex regulates excitatory synapse formation through AMPA receptor trafficking. GPC-2 regulates neurite outgrowth through PTP in dorsal root ganglia neurons (Coles et al., 2011). Other LAR-RPTP family proteins, LAR and PTP also bind to GPC-4 (Figure 23A). In addition to GPC-4, PTP also binds to cleaved form of GPC-2, GPC-3 and GPC-6 (Figure 23B). In future, it will be interesting to decipher exact cellular mechanisms of PTP /GPC-4/LRRTM4 complex in the regulation of synapse formation. Other interesting open questions are how other GPCs in combination with LAR-RPTPs contribute to synapse formation and transmission.

Figures and Legends

8. Figures and legends

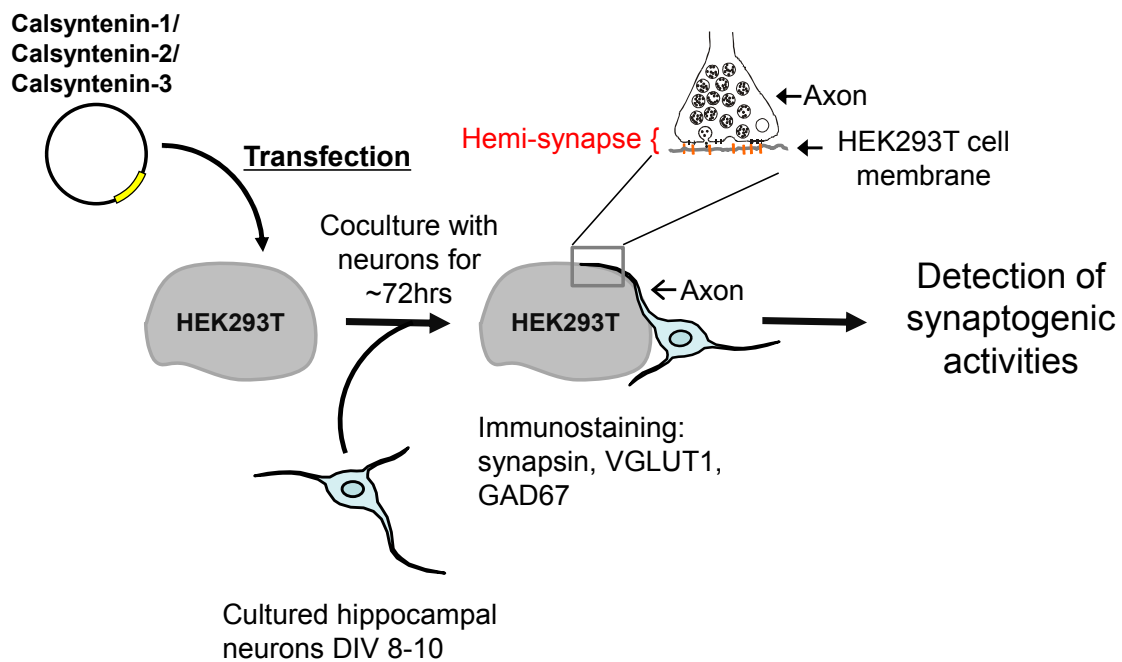


Figure 1. Schematic representation of heterologous synapse-formation assay. HEK293T cells were transfected with an expression vector for CST-1, CST-2, or CST-3. The transfected cells were co-cultured with cultured hippocampal neurons at DIV8-10. After 78 hours, sites of HEK293T cell contact with axons were analyzed for the accumulation of presynaptic proteins (Synapsin 1, VGLUT1, and GAD67). The co-cultured neurons formed hemi-synapses onto HEK293T cells expressing synapse organizers as depicted.

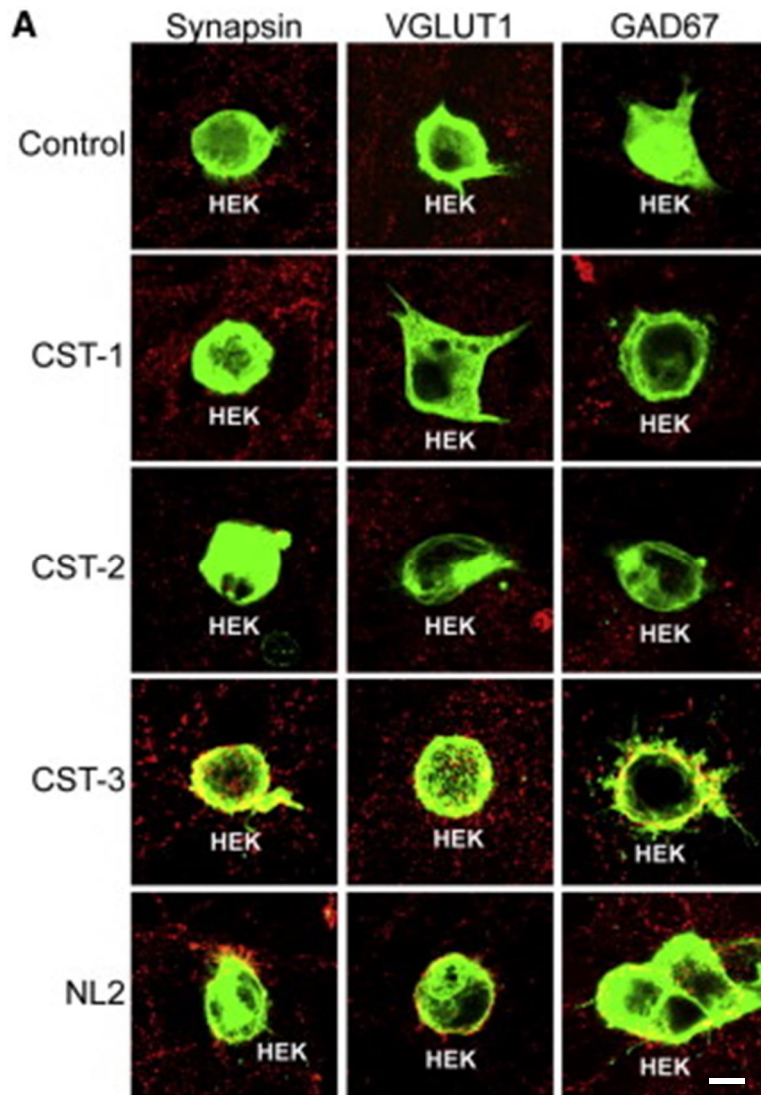


Figure 2. CST-3 induces presynaptic differentiation. HEK293T cells expressed EGFP alone or co-expressed EGFP and HA-CST-1, HA-CST-2, HA-CST3, or NL2-mVenus were co-cultured with rat hippocampal neuron at DIV 9-DIV 13. After 2-3 days, the cultured cells were immunostained with antibodies against Synapsin 1 (red), VGLUT1 (red) and GAD67 (red). Co-localization is shown in yellow. Scale bar represents 10 μ m.

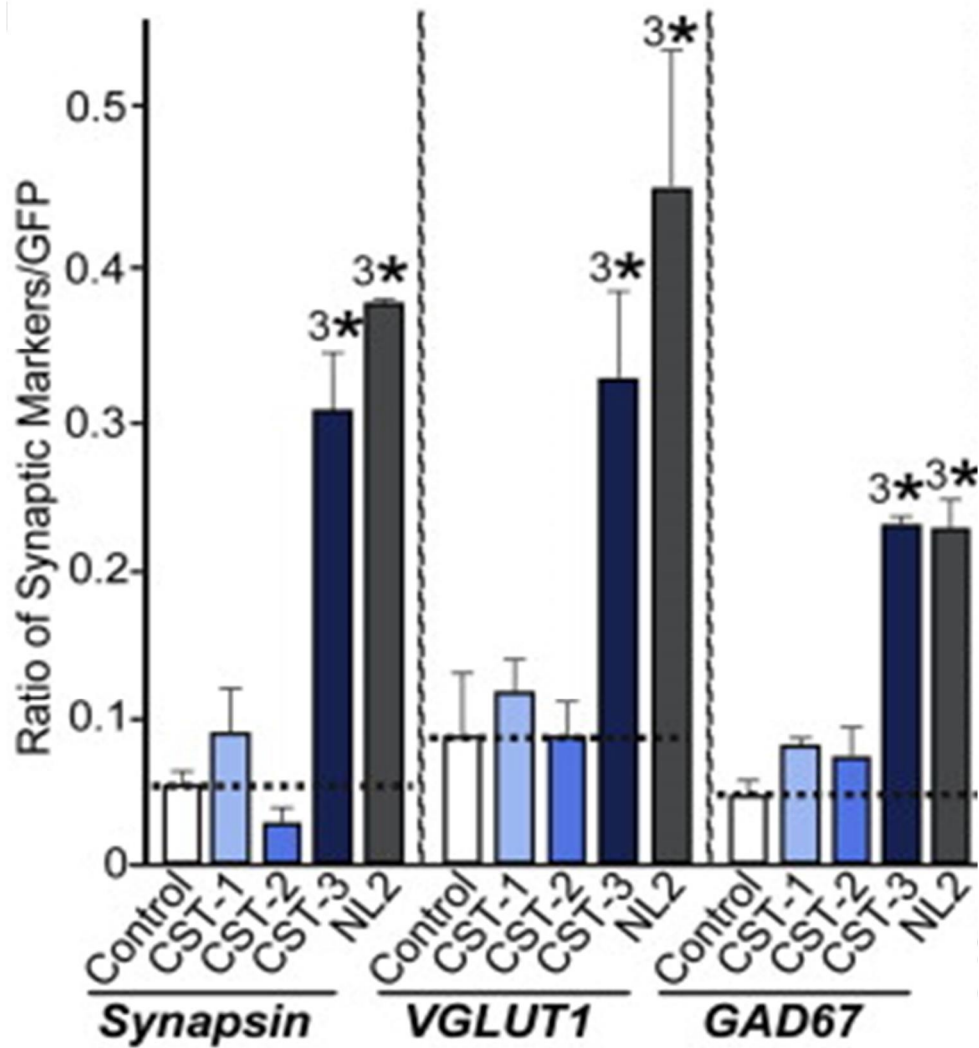


Figure 3. Quantification of the synaptogenic activities of CSTs in the heterologous synapse-formation assay. To quantify the experiments described in Figure 2, the ratio of the synaptic marker signal to EGFP signal was measured. The number of HEK293T cells analyzed was denoted as n : Control/Synapsin 1, $n = 18$; CST-1/Synapsin 1, $n = 21$; CST-2/Synapsin 1, $n = 17$; CST-3/Synapsin 1, $n = 16$; NL2/Synapsin 1, $n = 14$; control/VGLUT1, $n = 22$; CST-1/VGLUT1, $n = 17$; CST-2/VGLUT1, $n = 15$; CST-3/VGLUT1, $n = 15$; NL2/VGLUT1, $n = 16$; control/GAD67, $n = 15$; CST-1/GAD67, $n = 15$; CST2/GAD67, $n = 14$; CST-3/GAD67, $n = 15$; NL2/GAD67, $n = 14$. All values represent mean \pm SEM. 3*, $p < 0.001$; ANOVA with Turkey's test.

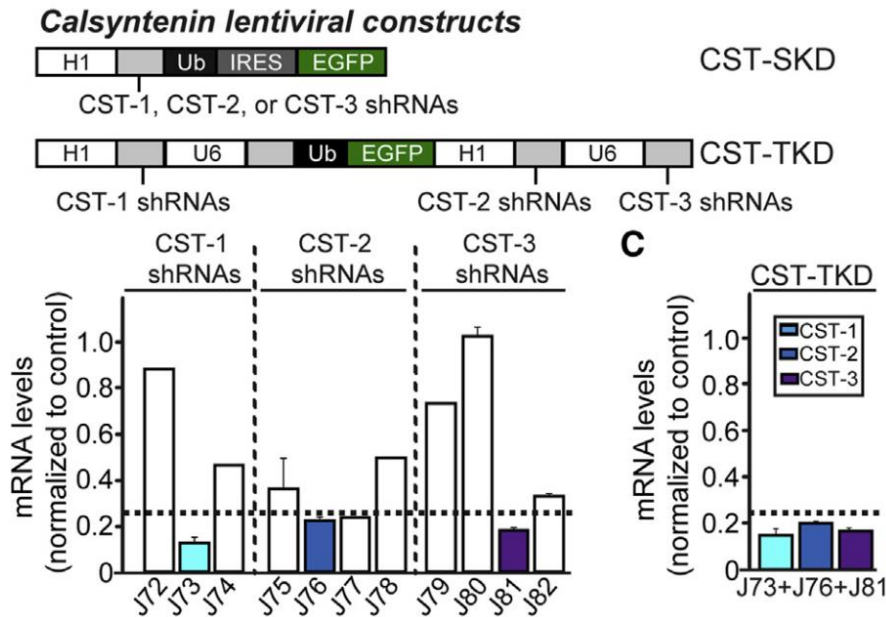


Figure 4. Quantification of knockdown efficiency of CSTs shRNA lentiviruses in cultured mouse cortical neurons. Schematic representation of lentiviral shRNA vectors for knockdown of single CST-1, CST-2 or CST-3 (CST-SKD), or triple knockdown of three CSTs (CST-TKD). CST-SKD vectors carry the CST-shRNA under the H1 promoter. CST-TKD vector carries the CST-1 and CST-2 shRNA under the H1 promoters and the CST-3 shRNA under the U6 promoter (upper panels). Expression levels of target mRNA of CSTs were analyzed by quantitative RT-PCR using cultured mouse cortical neurons infected at DIV3 with each CSTs shRNA lentivirus as indicated. For quantification, the mRNAs were prepared from infected cells at DIV12-13 (lower panels). Dotted lines represent 25% expression of specific mRNA.

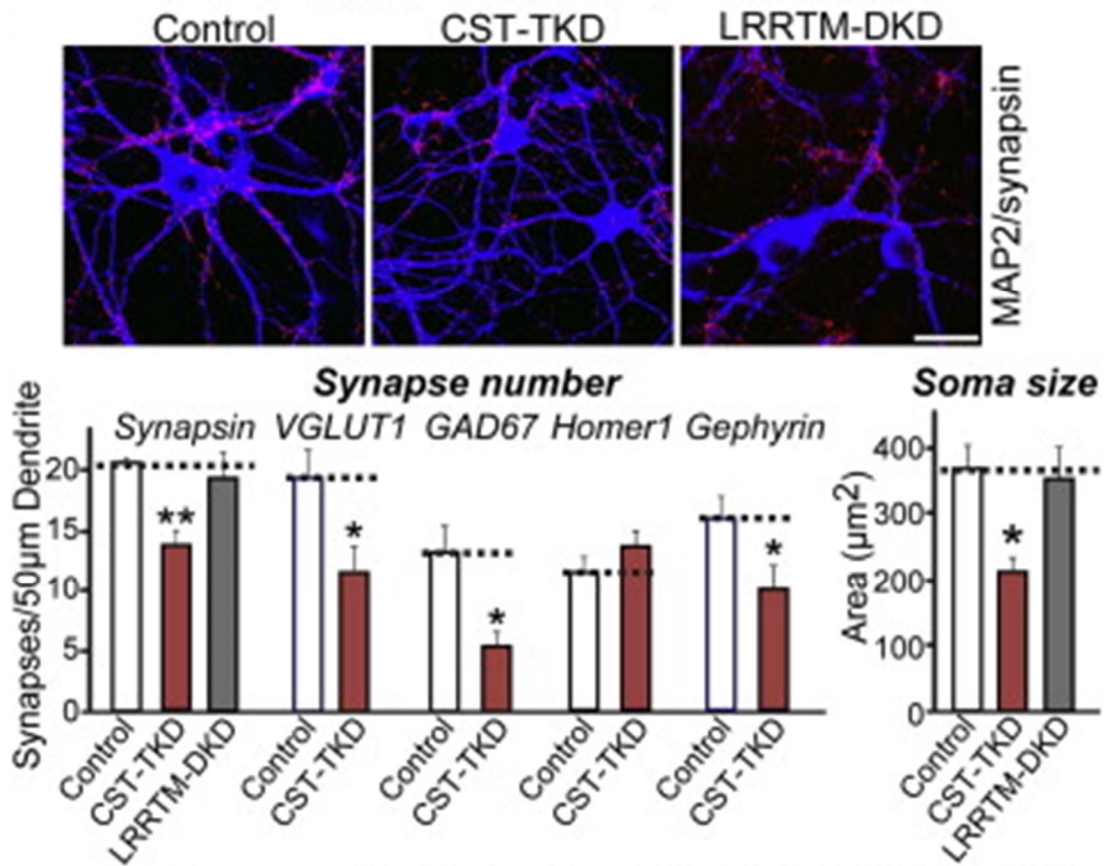


Figure 5. CST-TKD reduces synapse density and soma size in cultured mouse hippocampal neurons. (A) Representative images of cultured hippocampal neurons infected at DIV 3 with lentivirus expressing control shRNA, CST-TKD, or LRRTM-DKD (LRRTM1 and 2 double knockdown). The infected neurons at DIV14 were fixed and immunostained with antibodies against MAP2 (blue) and Synapsin 1 (red). Scale bar represents 35 μm. (B) Effects of CST-TKD on the densities of staining signals for Synapsin 1, VGLUT1, GAD67, Homer-1 and gephyrin. The number of neurons analyzed was denoted as \bar{n} : Control/Synapsin 1, $n = 16$; CST-TKD/Synapsin 1, $n = 18$; LRRTM-DKD/Synapsin 1, $n = 15$; control/VGLUT1, $n = 15$; CST-TKD/VGLUT1, $n = 15$; control/GAD67, $n = 15$; CST-TKD/GAD67, $n = 15$; control/Homer1, $n = 18$; CST-TKD/Homer1, $n = 21$; control/Gephyrin, $n = 22$; CST-TKD/Gephyrin, $n = 22$. (C) Effects of CST-TKD and LRRTM-DKD on the soma sizes. The soma size was measured using MAP2 signal. All values represent mean \pm SEM. 3^* , $p < 0.001$; ANOVA with Turkey's test.

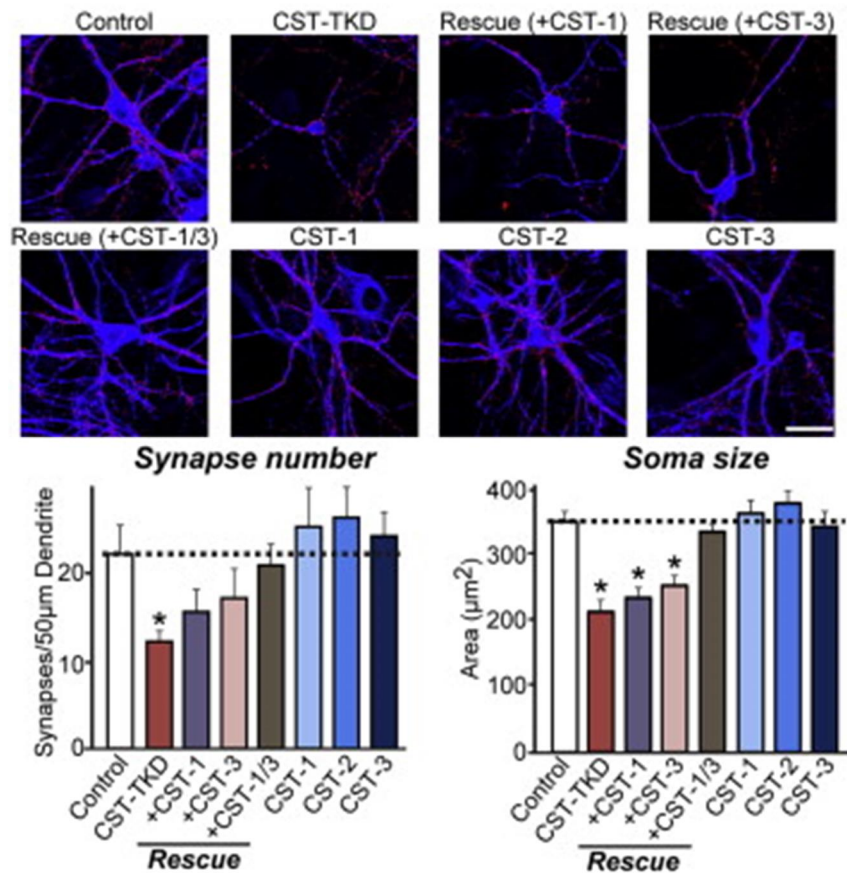


Figure 6. Effects of CST single knockdown on the synapse density and soma size in cultured mouse hippocampal neurons. (A) Representative images of cultured hippocampal neurons infected at DIV 3 with lentivirus expressing control shRNA, shRNA against CST-1-3 (CST-TKD), shRNA against CST-1 (CST-1), shRNA against CST-2 (CST-2), shRNA against CST-3 (CST-3), or CST-TKD together with human CST-1 [rescue (+CST-1)], CST-TKD together with human CST-3 [rescue (+CST-3)], CST-TKD together with human CST-1 and CST-3 [rescue (+CST-1/3)]. The infected neurons at DIV14 were fixed and immunostained with antibodies against MAP2 (blue) and Synapsin 1 (red). Scale bar represents 35 μm. (B and C) Effects of the indicated lentivirus on the density of staining signals for Synapsin 1 (B) and the soma size measured by MAP2 signal (C). The number of neurons analyzed was denoted as \bar{n} : Control, $n = 19$; CST-TKD, $n = 14$; CST-TKD + CST-1 rescue, $n = 15$; CST-TKD + CST-2 rescue, $n = 16$; CST-TKD + CST-3 rescue, $n = 17$; CST-TKD + CST-1/3 rescue, $n = 16$; CST-1, $n = 15$; CST-2, $n = 22$; CST-3, $n = 17$. All values represent mean \pm SEM. 3* , $p < 0.001$; ANOVA with Turkey's test.

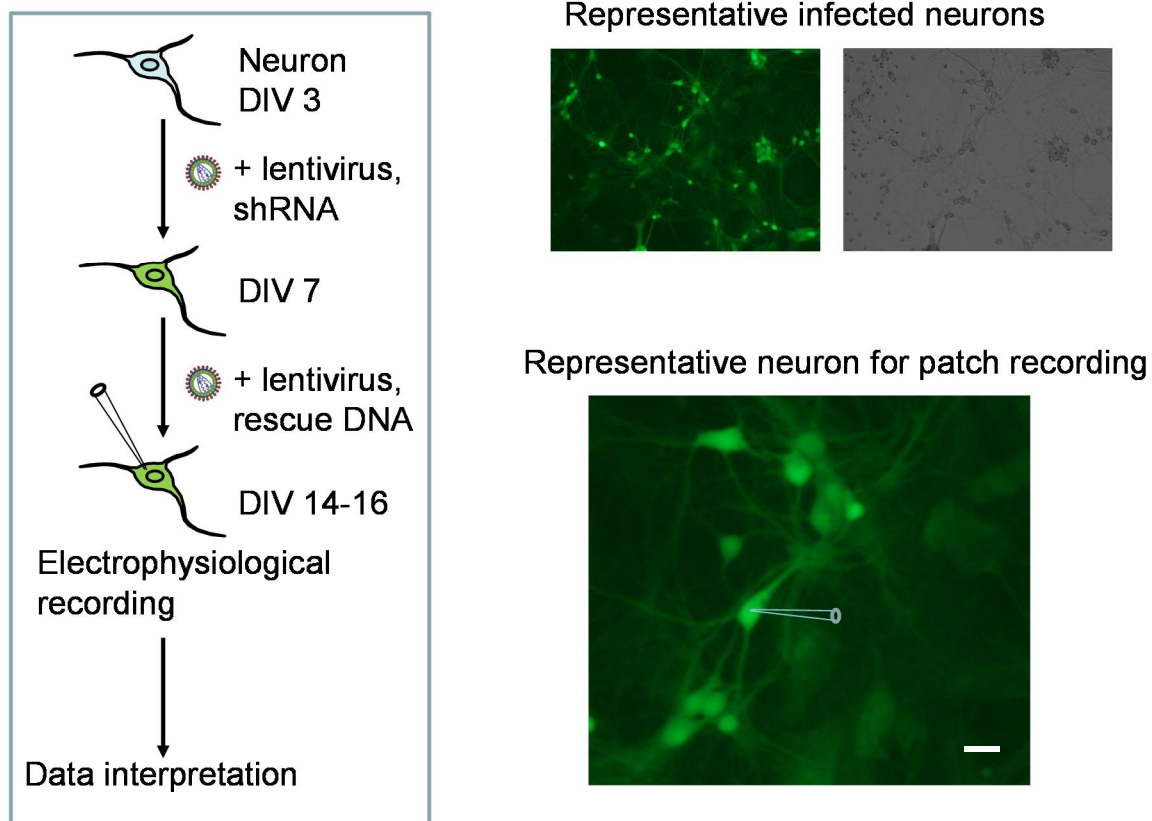


Figure 7. Experimental arrangement for electrophysiological recording of miniature postsynaptic currents (mEPSC/mIPSC) from cultured hippocampal neurons. In left panel: Cultured hippocampal neurons were infected with lentivirus containing shRNA at DIV 3, and were infected with lentivirus containing rescue construct at DIV 7. Electrophysiological recording was performed at DIV 14-16 for analysis of mEPSC/mIPSC. Right upper panels represent cultured neurons infected with EGFP containing lentivirus shown in green; Right lower panel represents pyramidal cell selected for electrophysiological recording. Scale bar represents 50 μm .

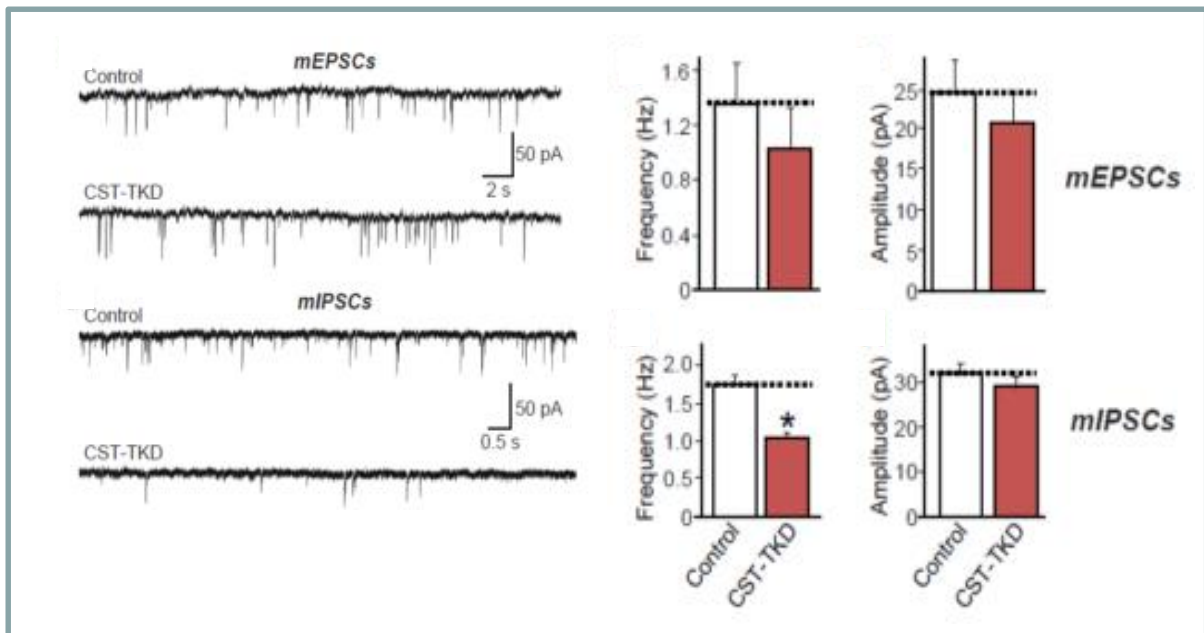


Figure 8. CST-TKD impairs inhibitory synaptic transmission in cultured hippocampal neurons. Above diagram is depicted as follows: left panels represent mEPSCs/mIPSC traces, right upper panels represent mEPSCs frequency and amplitudes, right lower panels represent mIPSCs frequency and amplitude. Cultured hippocampal neurons were infected with lentiviruses expressing control shRNA or CST-TKD (sh-CST-1, sh-CST-2, and sh-CST-3) at DIV 3. Excitatory and inhibitory postsynaptic transmissions were measured at DIV 14-16. Here $\bar{x} \pm \text{SEM}$ denotes number of neurons analyzed. sh-control, $n = 24$; CST-TKD, $n = 22$. All values represent mean \pm SEM. *, $p < 0.05$; student's t test.

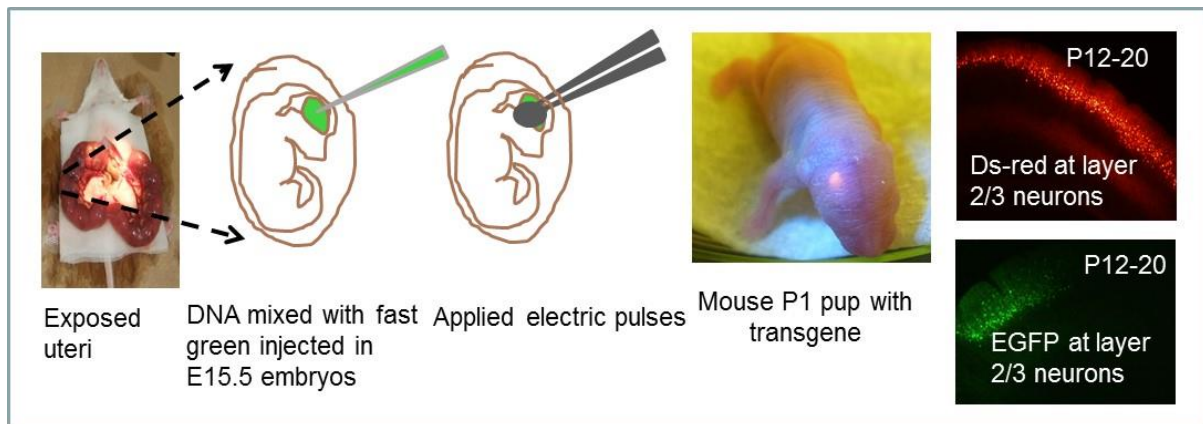


Figure 9. Procedure for in utero electroporation to introduce DNAs in the pyramidal neurons in layer 2/3 cerebral cortex. **Step1-** Uteri were exposed and wetted with PBS. **Step2-** DNA mixture was injected in the lateral ventricle. **Step3-** Electrical pulses were applied. **Step4-** Operation was completed within 30 min. **Step5-** Mouse was placed on 37 °C plate for recovery, returned back to the home cage and kept until natural delivery. **Step6-** Expression of transgene was examined with LED penlight. A signal is shown as a red spot on the head of mouse P1 pup in the picture. **Step7-** Gene transfected mice were used for acute brain slice preparation for electrophysiological recording. Ds-red and EGFP signals in the transfected pyramidal neurons in layer 2/3 cerebral cortex were shown in acute brain slices of P12-P20 mice.

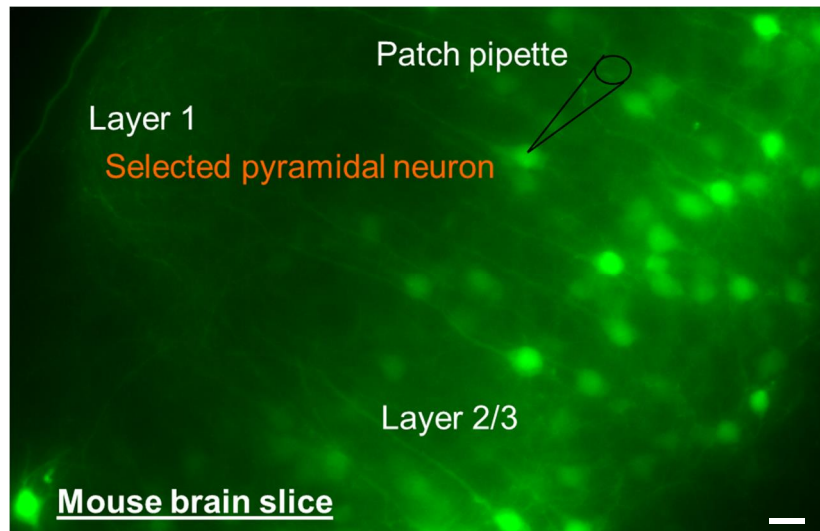
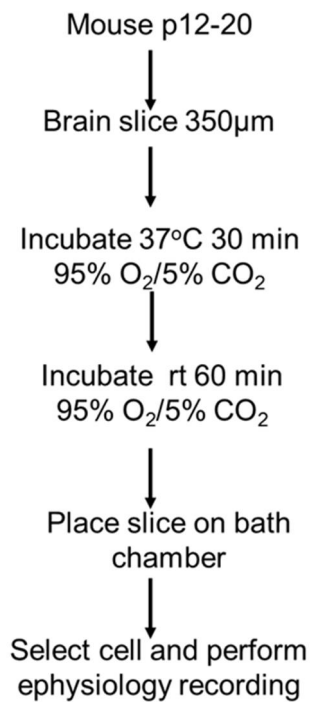


Figure 10. Experimental arrangement for slice electrophysiology. E15.5 mouse embryos were in utero electroporated to introduce control shRNA or CST-TKD (sh-CST-1, sh-CST-2, and sh-CST-3) together with EGFP as a fluorescent marker. P12-20 transfected mice were used for coronal brain slice preparation. Left: Brief description of coronal brain slice preparation. Right: Representative brain slice showing distribution of transgene expressing neurons in the pyramidal neurons in layer 2/3 cerebral cortex. Scale bar represents 150 μm.

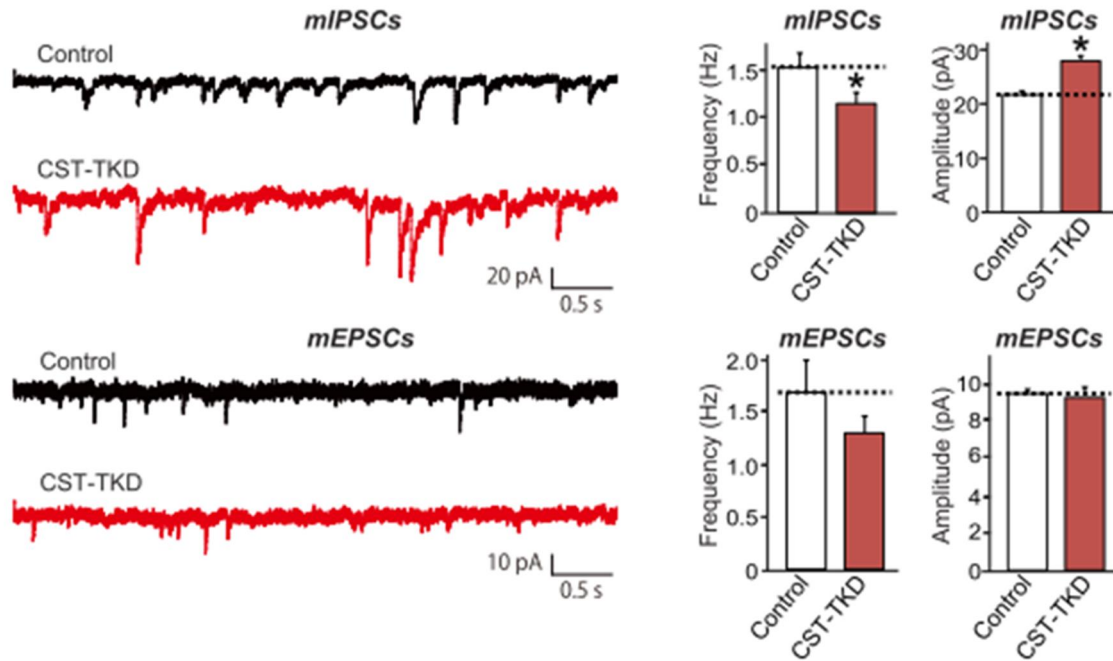


Figure 11. CST-TKD impairs inhibitory synaptic transmission in the pyramidal neurons in layer 2/3 cerebral cortex in mice. Miniature postsynaptic currents (mIPSCs/mEPSCs) were measured from control and CST-TKD (sh-CST-1, sh-CST-2, and sh-CST-3) layer 2/3 cortical pyramidal neurons. Left: Representative electrical traces for mIPSCs and mEPSCs. Right: mIPSCs frequency and amplitude (above), and mEPSCs frequency and amplitude (below). Here n denotes number of neurons analyzed. mIPSCs control, $n = 10$; mIPSCs CST-TKD, $n = 12$; mEPSCs control, $n = 29$; mEPSCs CST-TKD, $n = 30$. All values represent mean \pm SEM. *, $p < 0.05$; student's t test.

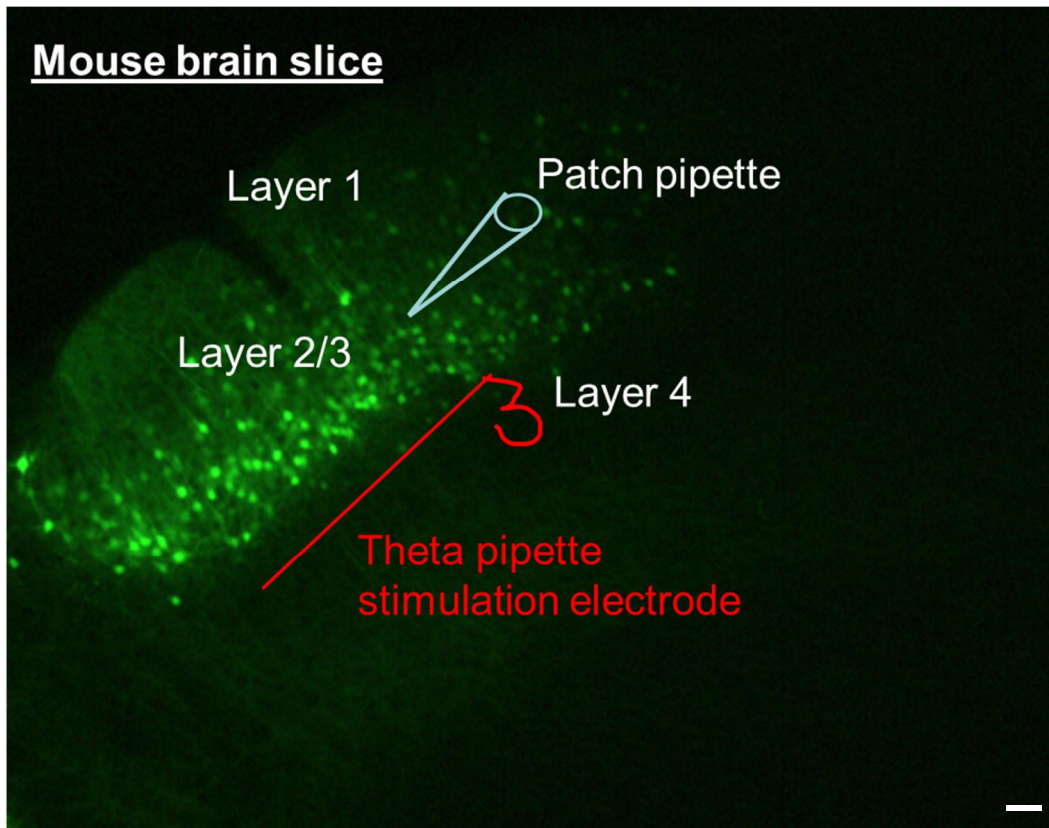


Figure 12. Experimental arrangement for slice electrophysiological stimulation. E15.5 mouse embryos were in utero electroporated with control shRNA or CST-TKD (sh-CST-1, sh-CST-2, and sh-CST-3) together with EGFP as a fluorescent marker. P12-20 transfected mice were used for coronal brain slice preparation. The image depicted experimental arrangement for electrical stimulation and paired-pulses ratios (PPR) recording. Neurons expressing transgenes in layer 2/3 cerebral cortex are shown. Theta glass stimulation pipette (shown as red) filled with extracellular solution was placed on layer 4 cerebral cortex, and layer 2/3 pyramidal neurons were patched (shown light blue pipette) and PPRs were recorded. Scale bar represents 250 μm .

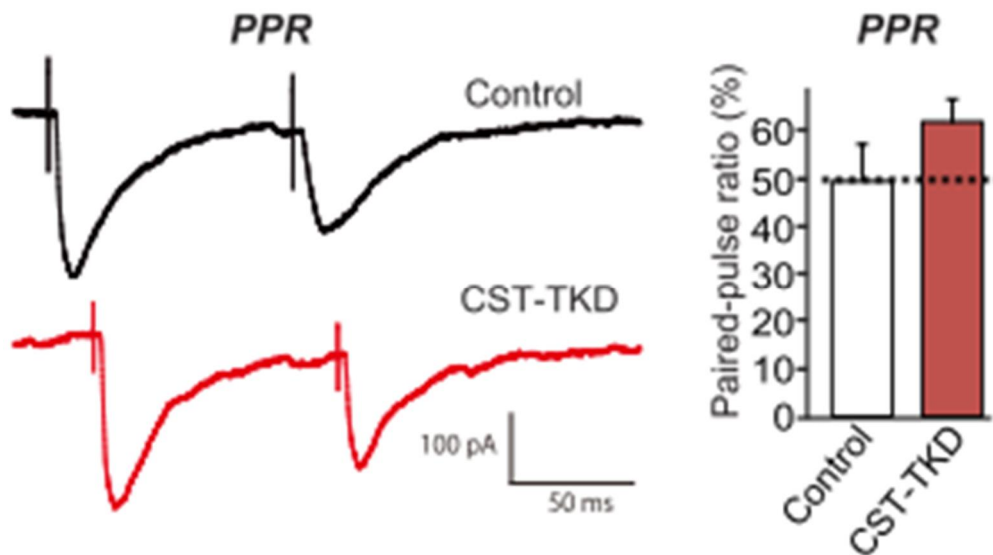


Figure 13. CST-TKD does not impair inhibitory postsynaptic paired-pulse ratio (IPSC-PPR) in layer 2/3 cerebral cortex in mice. E15.5 mouse embryos were in utero electroporated with control shRNA or CST-TKD (sh-CST-1, sh-CST-2, and sh-CST-3) together with EGFP as a fluorescent marker. P12-20 transfected mice were used for coronal brain slice preparation. Theta glass stimulation pipette filled with extracellular solution was placed on layer 4 cortex, and layer 2/3 pyramidal neurons were patched (shown light blue pipette) and PPRs were recorded. Left: Representative traces for control IPSC-PPR and CST-TKD IPSC PPR. Here \bar{n} denotes number of neurons analyzed. IPSCs PPR control, $n = 13$; IPSCs PPR CST-TKD, $n = 15$. All values represent mean \pm SEM. *, $p < 0.05$; student's t test.

Accession number	Gene Name	Protein description	Mascot Score	Peptide Matches
Q9CS84	Nrx-1	neurexin-1	130	59
Q63374	Nrx-2	neurexin-2	26	29
Q6P9K9	Nrx-3	neurexin-3	70	48

Table 1. Identification of Nrx- as potential interaction partners for CST-3 by LC/MS/MS.

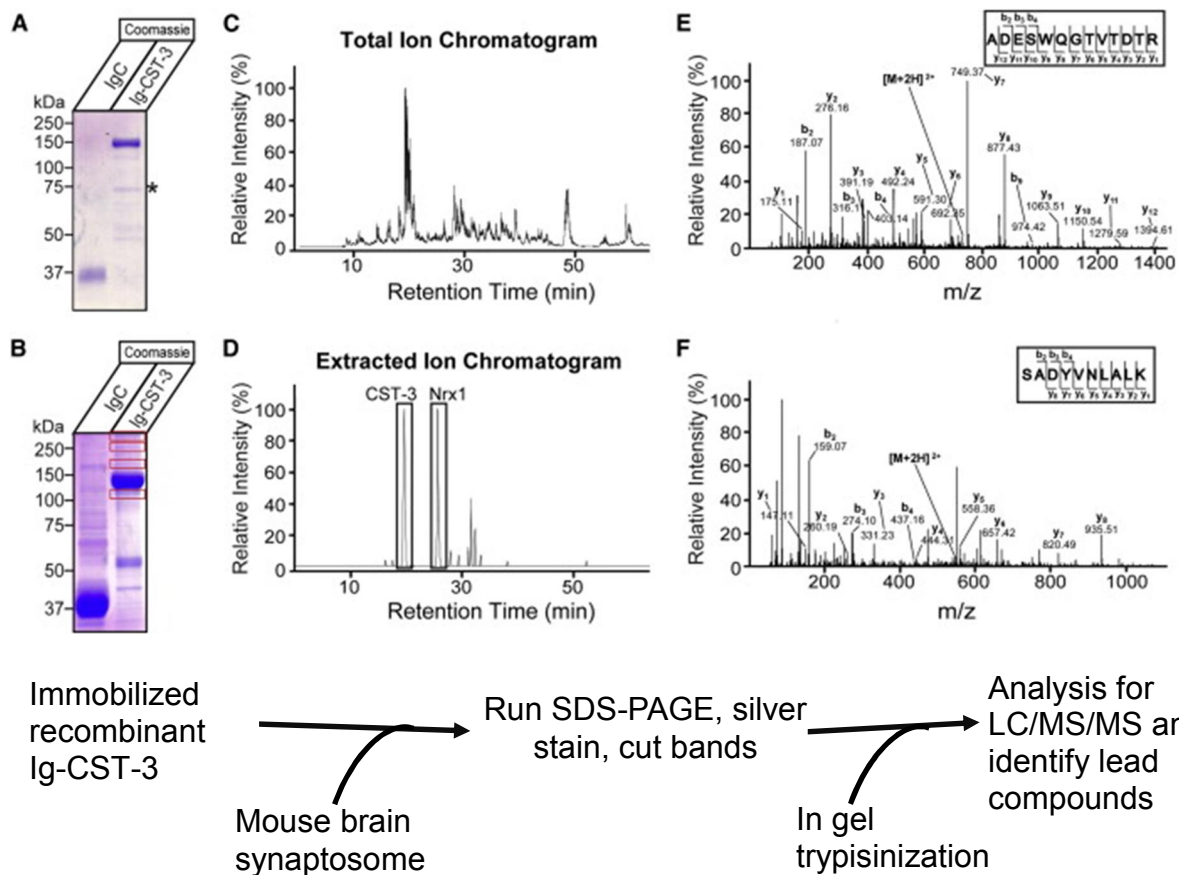


Figure 14. Identification of CST-3 interacting molecules. Identification of potential CST-3 (Ig fused CST-3, Ig-CST-3) binding partners was performed by affinity chromatography followed by SDS-PAGE separation, liquid chromatography and tandem mass spectrometry. (A) SDS-PAGE analysis of soluble control Ig (IgC) and Ig fused CST-3. (B) Mouse brains were homogenized and soluble brain proteins were incubated with protein A Sepharose bound to IgC or Ig-CST-3 at 4 °C overnight. Equivalent amount of IgC and Ig-CST-3 were separated in SDS-PAGE and were stained with Coomassie blue stained. Unique bands were cut and analyzed by mass spectrometry. (C) Total ion chromatogram separated band. (D) Extracted ion chromatogram showing CST-3 (CST-3, retention time = 19.30 min) and Nr-1 (Nr1, retention time = 25.77 min). (E) Mass to charge ratio (m/z) for CST-3 was 733.33 and representative peptide sequence obtained ADESWQGTVDTR (amino acid sequence 684-696). (F) Mass to charge ratio (m/z) for Nr-1 was 547.29 and representative peptide sequence obtained SADYVNLALK (amino acid sequence 327-336). Flow diagram shows brief schematics of identification of CST-3 interaction partners.

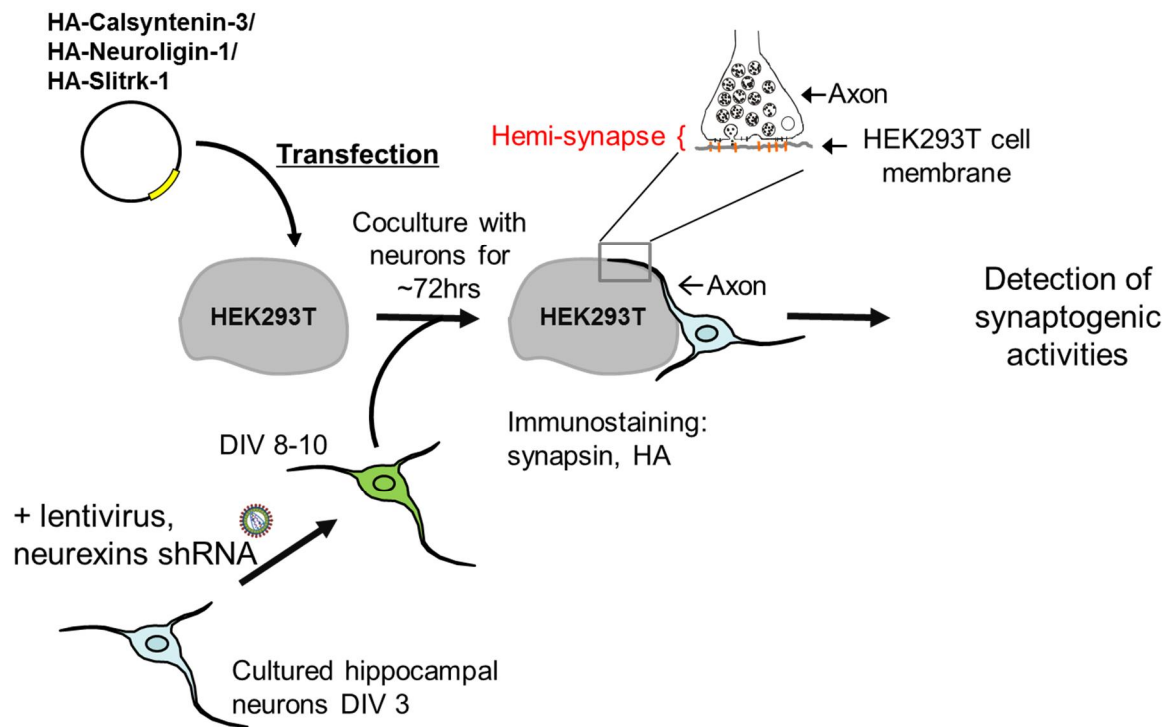


Figure 15. Schematic representation of heterologous synapse-formation assay. HEK293T cells were transfected with an expression vector for HA-CST-3, HA-NL1, or Slitrk1. The transfected HEK293T cells were added to cultured hippocampal neurons (DIV 8-10) infected with lentivirus expressing sh-Nrxn1/2/3. After 72 hours of co-culture, sites of HEK293T cell contact with axons were analyzed for the accumulation of presynaptic proteins (Synapsin 1) and HA-tag signal. The co-cultured neurons formed hemi-synapse onto HEK293T cells expressing synapse organizer as depicted.

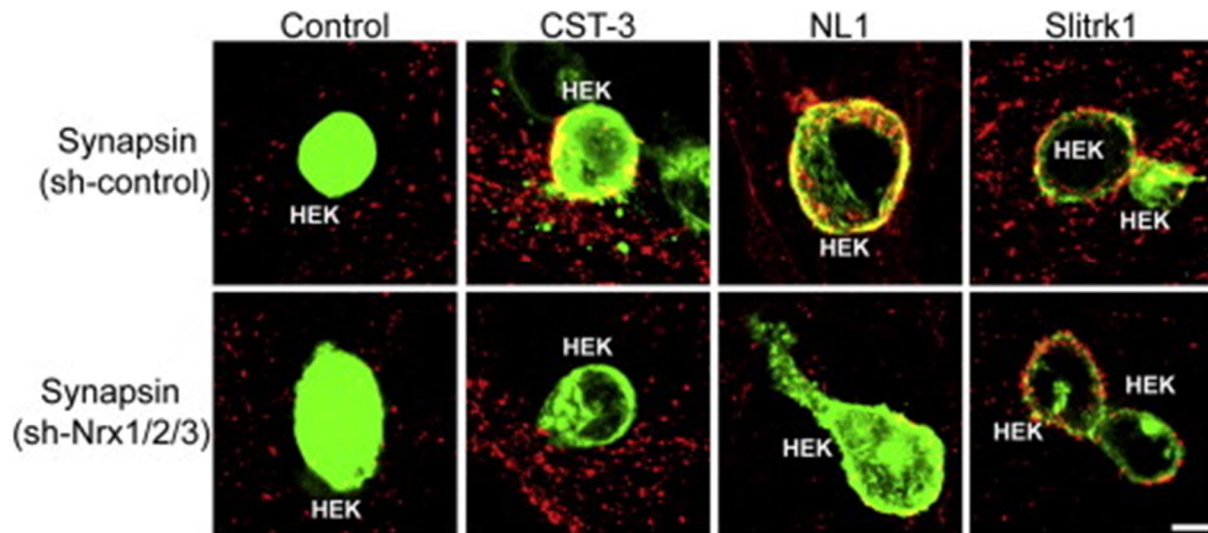


Figure 16. Nrxs are essential for CST-3-mediated presynaptic differentiation. The cultured mouse hippocampal neurons were infected with lentivirus expressing sh-Nrxn1/2/3. The infected neurons were co-cultured with HEK293T cells expressing HA-CST-3, NL1-mVenus, or Slitrk1. After 72 days of co-culture, the cells were fixed and immunostained with antibodies against mVenus (green) or HA-tag (green) and Synapsin 1 (red). Scale bar represents 10 μ m.

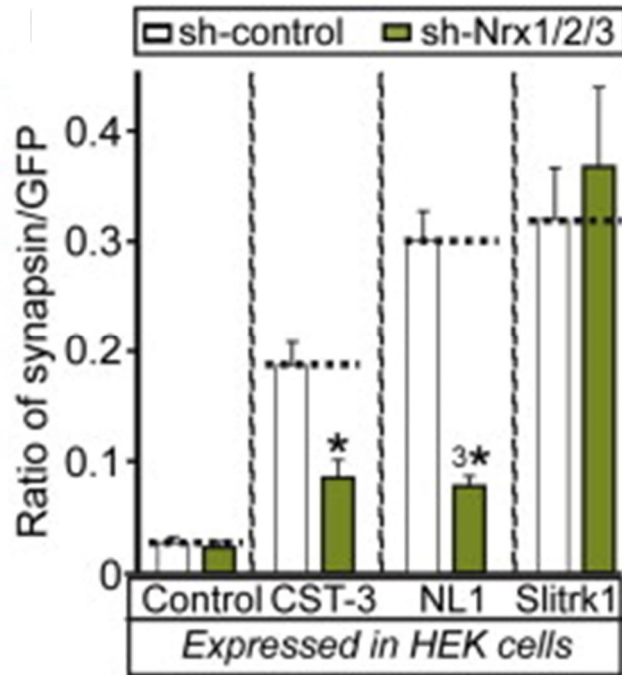


Figure 17. Quantification of the effect of Nr_x triple knockdown on the synaptogenic activity of CST-3. To quantify the experiments described in Figure 16, the ratio of the synaptic marker signal to EGFP, mVenus, or HA signal was measured. The number of HEK293T cells analyzed is indicated as n: Control/sh-control, n = 19; CST-3/sh-control, n = 43; NL1/sh-control, n = 30; Slitrk1/sh-control, n = 24; control/sh-Nr_x-1/2/3, n = 45; CST-3/sh-Nr_x-1/2/3, n = 39; NL1/sh-Nr_x-1/2/3, n = 28; Slitrk1/sh-Nr_x-1/2/3, n = 29. All values represent mean ± SEM. 3* and *, p < 0.001 and p < 0.05, respectively; ANOVA with Turkey's test.

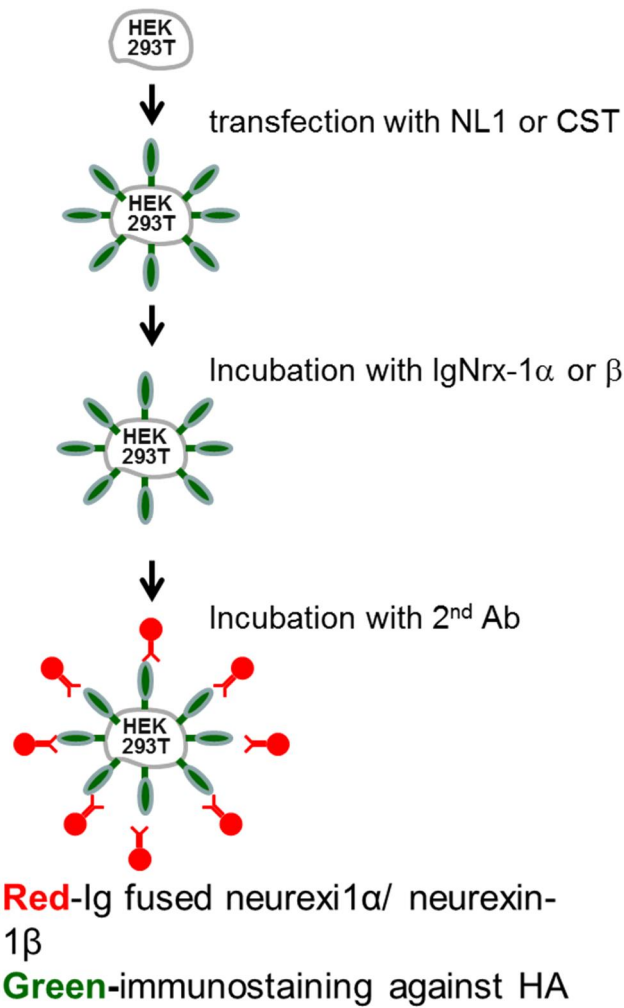


Figure 18. Schematic representation of cell surface binding assay. HEK293T cells were transfected with expression vectors for indicated proteins. The transfected cells were incubated with 0.2 μ M purified Ig fusion proteins. After washing and fixation, the cells were incubated with fluorescence-labeled anti-Ig (red) and anti-HA antibodies to detect the binding.

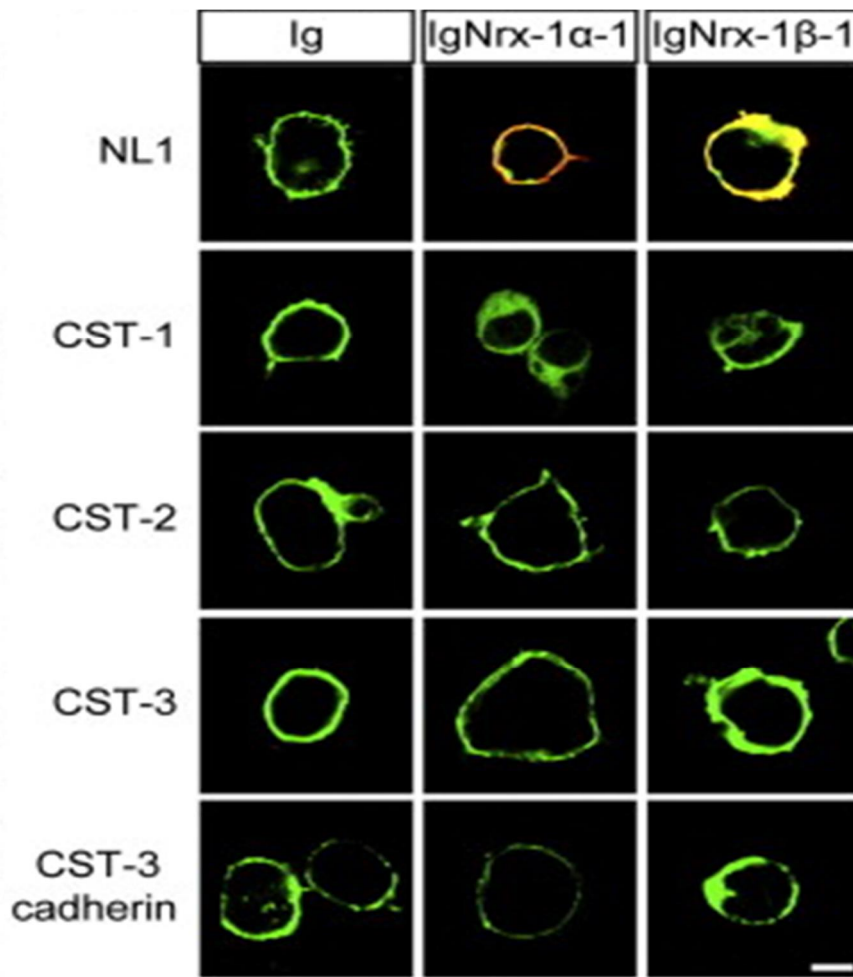


Figure 19. CST-3 does not directly bind to Nrxs. HEK293T cells were transfected with an expression vector for HA-NL1, HA-CST-3, HA-CST-2, or HA-CST-3. The transfected cells were incubated with purified Ig-Nrx-1 or Ig-Nrx-1 . After washing, cells were immunostained with antibodies against HA-tag (green) and Ig (red). Scale bar represents 10 μ m.

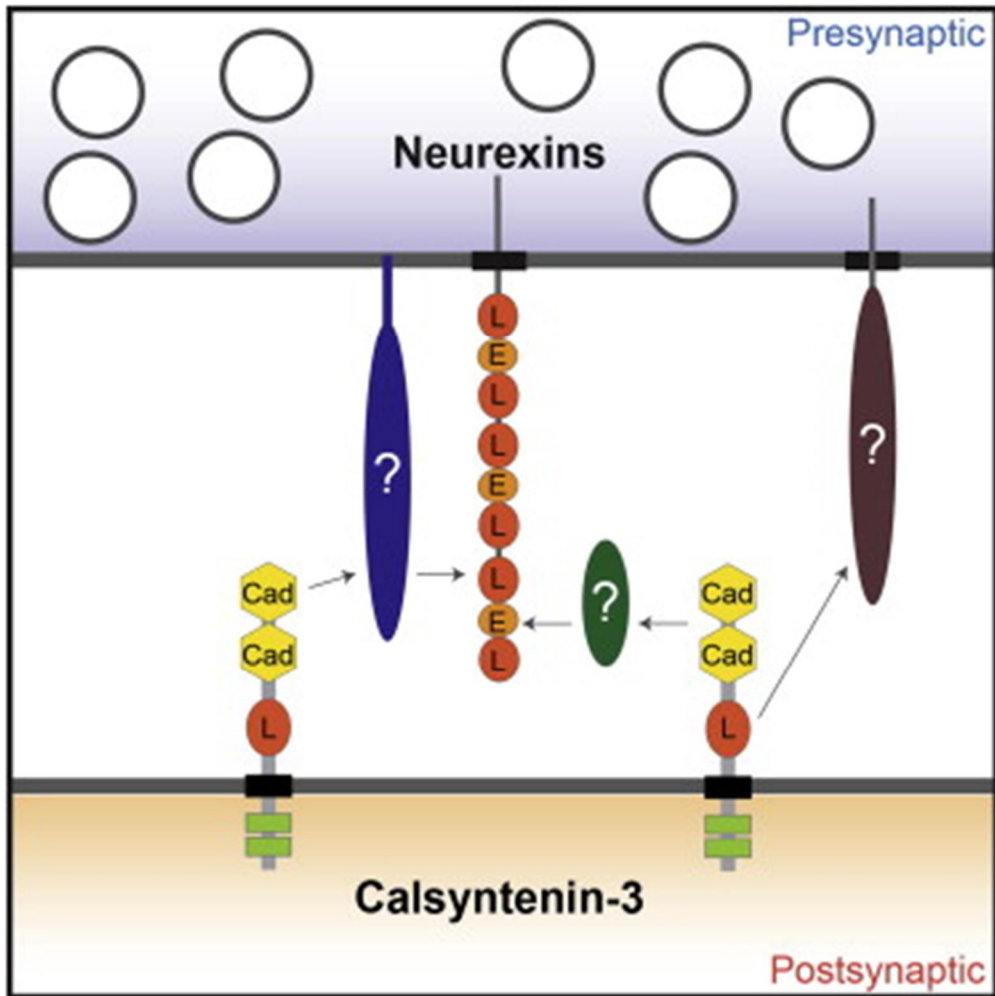


Figure 20. A proposed model for trans-synaptic interaction between presynaptic Nrxs and postsynaptic CST-3 through unidentified protein. In this model, CST-3 interacts with Nrnx through unidentified co-receptor of Nrnx or soluble protein.

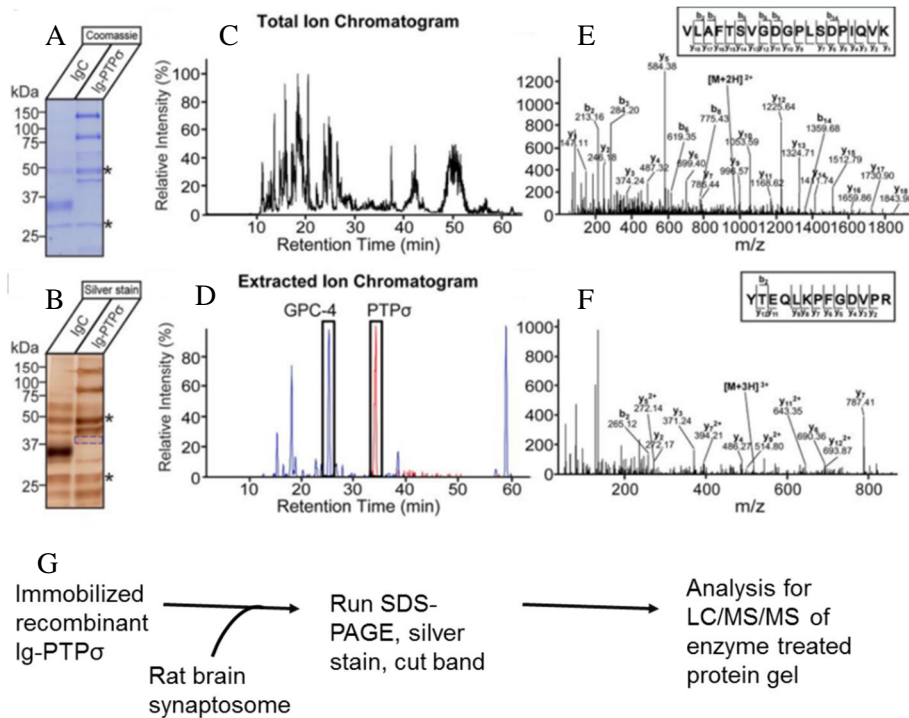


Figure 21. Identification of PTP binding partners by affinity chromatography. (A) Purified recombinant IgC and IgC-PTP were resolved in SDS-PAGE gel and Coomassie blue stained. (B) Mouse brains were homogenized and soluble brain proteins were incubated with immobilized IgC or Ig-PTP on Protin A Sepharose at 4 °C for overnight. Equivalent amount of pulled down proteins were separated in SDS-PAGE and Coomassie blue stained. Unique bands were cut and analyzed by mass spectrometry. Asterisks (*) in $\delta A \delta$ and $\delta B \delta$ indicate cleaved PTP or IgC heavy chains. (C) Total ion chromatogram of separated band. (D) Extracted ion chromatogram showing glypican-4 (GPC-4, retention time = 24.88 min) and PTP (retention time = 34.05 min). (E) Mass to charge ratio (m/z) for GPC-4 was 517.28 and representative peptide sequence obtained YTEQLKPFQDVPR. (F) Mass to charge ratio (m/z) for PTP was 972.03 and representative peptide sequence obtained VLAFTSVGDGPLSDPIQVK. (G) Procedure for the experiment describe in this Figure.

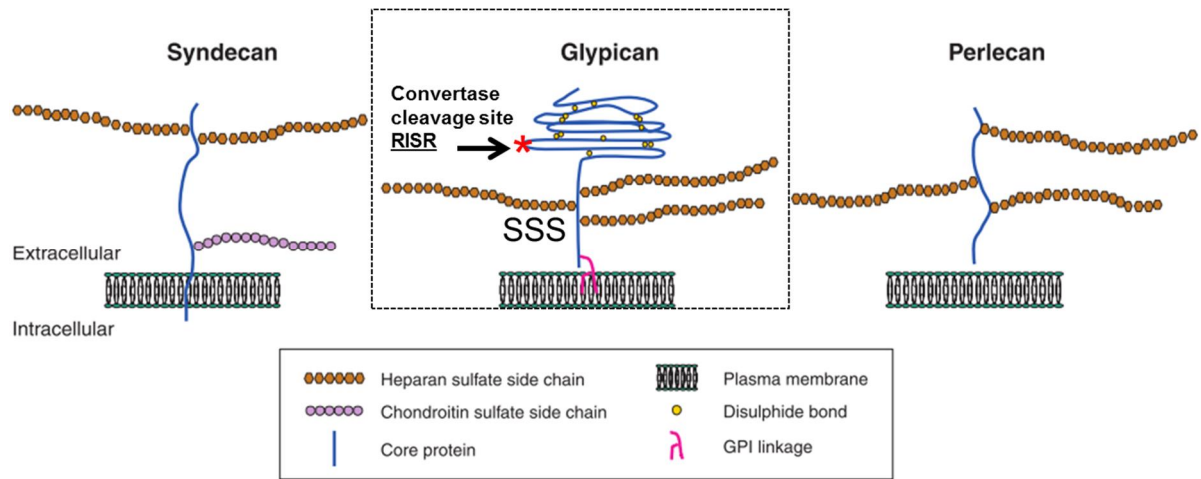


Figure 22. Glypicans (GPCs) are heparan sulfate proteoglycans that bind to the outer surface of the plasma membrane by a glycosylphosphatidylinositol (GPI) anchor. There are six mammalian GPCs; GPC1-6. GPCs have conserved cleavage site δ RISR δ and heparan sulfate binding site δ SSS δ (Lin X 2004).

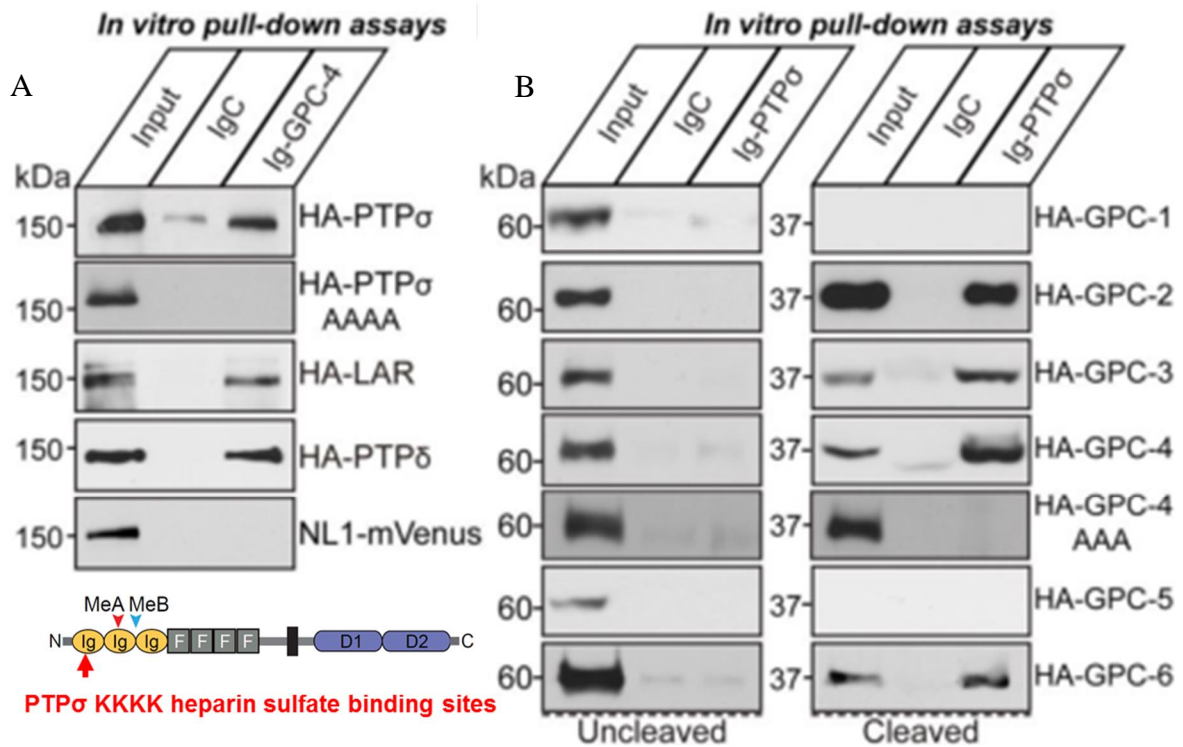


Figure 23. PTP σ interacts with cleaved GPC4 through immunoglobulin (Ig). (A) Pull-down assays were performed with purified IgC and Ig-GPC-4 by using HEK293T cells lysates expressing indicated proteins. Mixtures of cell lysates and Ig proteins were precipitated with protein A-sepharose beads, followed by immunoblotting with anti-HA antibody. (B) Pull-down assays were performed with purified IgC and Ig-PTP σ by using HEK293T cell lysates expressing indicated proteins. Mixtures of cell lysates and Ig proteins were precipitated with protein A-sepharose beads, followed by immunoblotting with anti-HA antibody. Immunoblot detected ~65 kDa of full length GPC (Left) and ~37 kDa of cleaved GPC (Right).

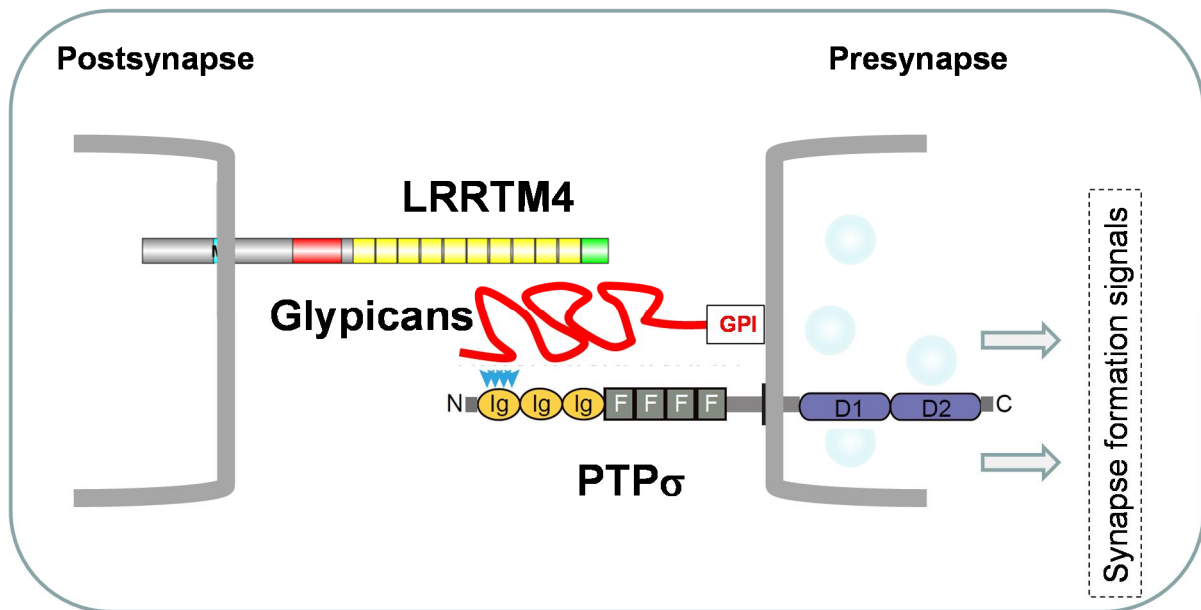


Figure 24. A proposed model for LRRTM4/GPCs/PTP σ complex. LRRTM4 is located in postsynaptic membrane. PTP and GPI-anchored GPCs are in the presynaptic terminals. LRRTM4, GPCs and PTP form trans-synaptic protein complex and regulate synapse formation.

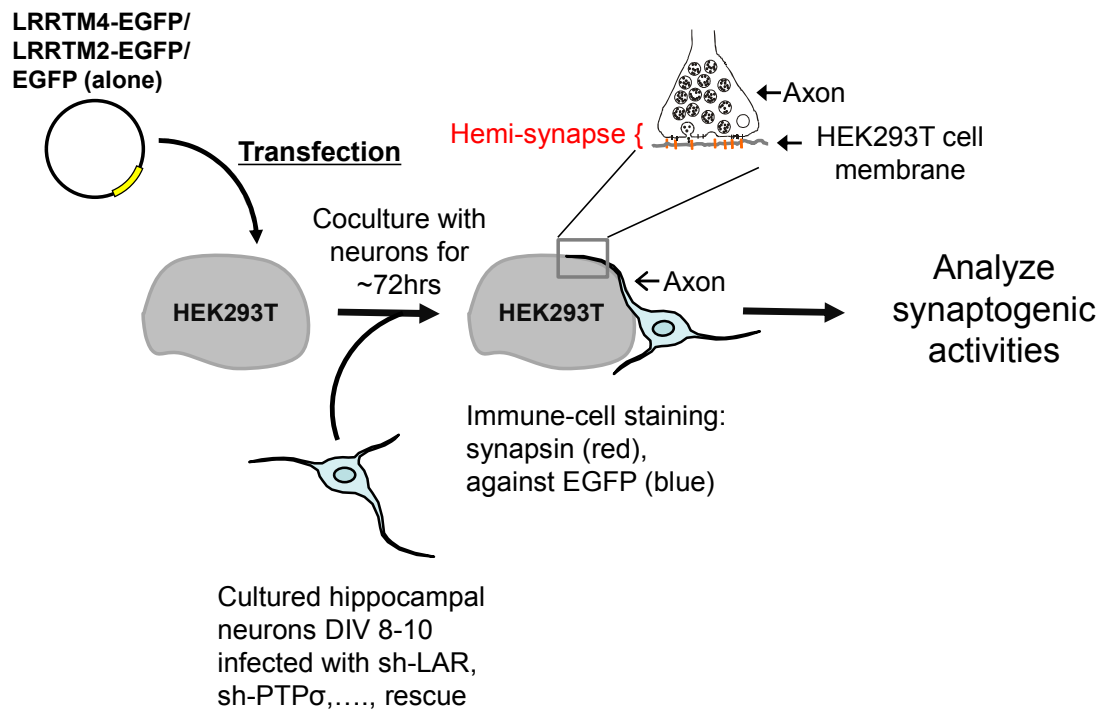


Figure 25. Schematic representation of heterologous synapse-formation assay. HEK293T cells transfected with either LRRTM4-EGFP, LRRTM2-EGFP, or EGFP were added to cultured hippocampal neurons infected with lentivirus containing sh-LAR, sh-PTP , and wild-type rescue constructs for PTP at DIV 8-10 and co-cultured for 72 hours. Co-cultured neurons form hemi-synapse onto HEK293T cells as depicted. Neurons were immunostained at DIV 14 with antibodies for GFP. Confocal images were taken to analyze synaptogenic activities.

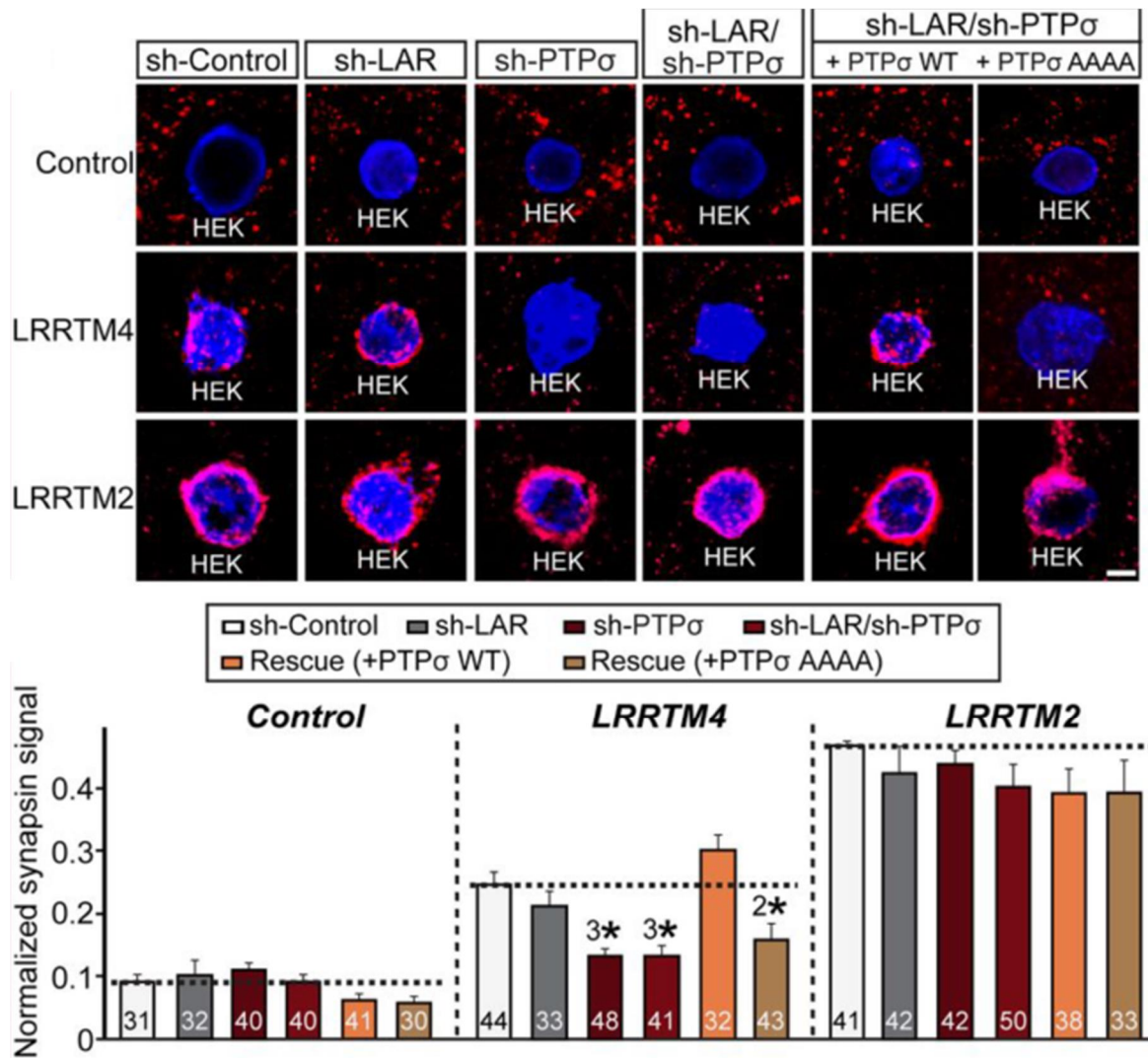


Figure 26. PTP is required for LRRTM4-mediated presynaptic differentiation. Neurons were infected with lentiviruses expressing following shRNA or together with rescue constructs: sh-control, sh-LAR, sh-PTP, sh-LAR sh-LAR/sh-PTP, sh-LAR/sh-PTP + PTP WT rescue, or sh-LAR/sh-PTP + PTP -A4A4A rescue. HEK293T cells were transfected with LRRTM4-EGFP, LRRTM2-EGFP, or EGFP and co-cultured with lentiviruses infected neurons. Co-cultured cells were immunostained against EGFP (blue) and Synapsin 1 (red). Representative images in different conditions were shown in upper panel. Co-localizations were indicated in violet color surrounding HEK293T cells. Scale bar represents 25 μ m. All values represent mean \pm SEM. 3* and *, $p < 0.001$ and $p < 0.01$, respectively; ANOVA with Turkey's test. The number of HEK293T cells analyzed is indicated in each bar graph.

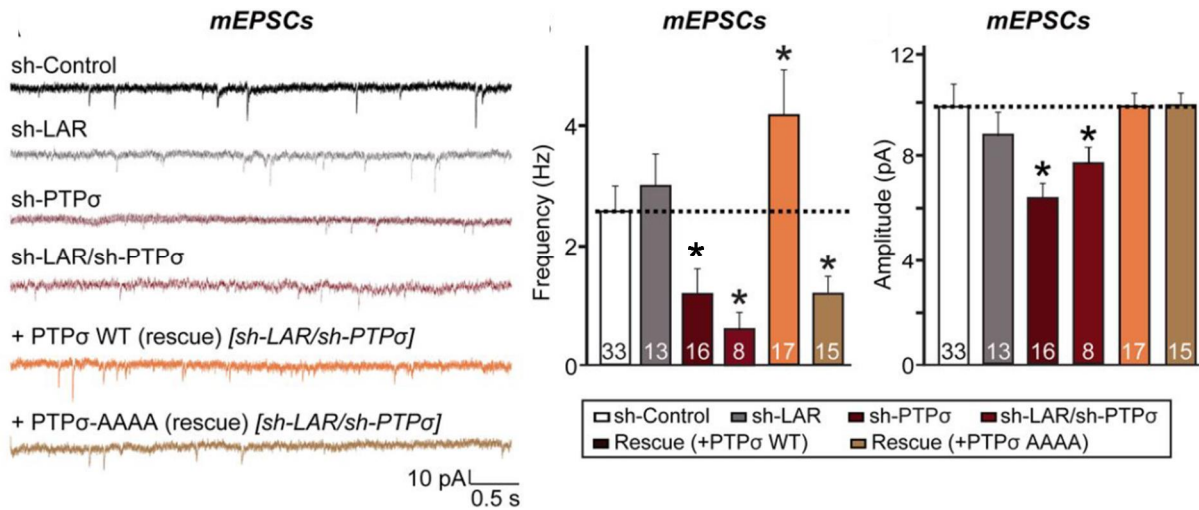


Figure 27. PTP regulates excitatory synaptic transmission through heparan sulfate interaction. Above diagram depicted as following: left representative mEPSC traces, middle mEPSCs frequency and right mEPSCs amplitudes. Cultured hippocampal neurons were infected with lentiviruses expressing following combination of shRNAs or together with rescue constructs: sh-control, sh-LAR, sh-PTP, sh-LAR, sh-LAR/sh-PTP, sh-LAR/sh-PTP + PTP WT rescue, or sh-LAR/sh-PTP + PTP -AAAA rescue. First infections were performed at DIV 3 and rescued infections were performed at DIV 7, and excitatory postsynaptic transmission was measured at DIV 14-16. All values represent mean \pm SEM. *, $p < 0.05$; student's t test. The number of neurons analyzed is indicated in each bar graph.

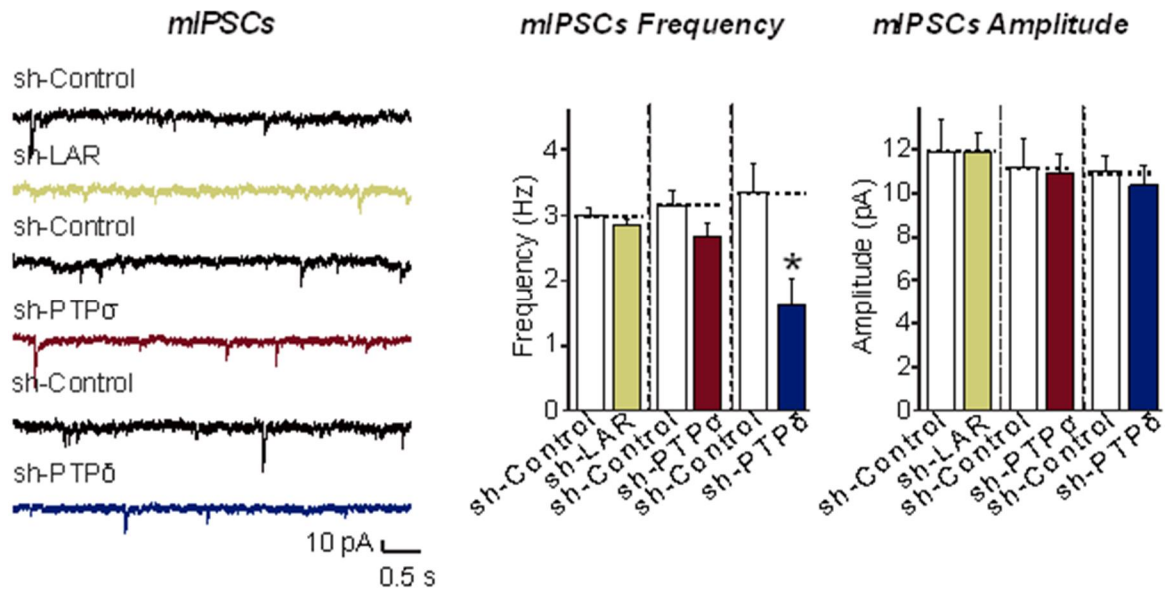


Figure 28. Knockdown of PTP δ does not change inhibitory synaptic transmission in cultured hippocampal neurons. Above diagram depicted as following: left representative mIPSC traces, middle mIPSCs frequency and right mIPSCs amplitudes. Cultured hippocampal neurons were infected at DIV 3 with lentiviruses expressing following shRNAs constructs: sh-control, sh-LAR, sh-PTP σ , or sh-PTP δ . Inhibitory postsynaptic transmission was measured at DIV 14-16. Data represented as Mean \pm SEM (*, $p < 0.05$, student's t test). Here n denotes number of neurons analyzed. sh-control, $n = 13$, sh-LAR, $n = 13$; sh-control, $n = 14$, sh-PTP σ , $n = 20$; sh-control, $n = 17$, sh-PTP δ , $n = 12$.

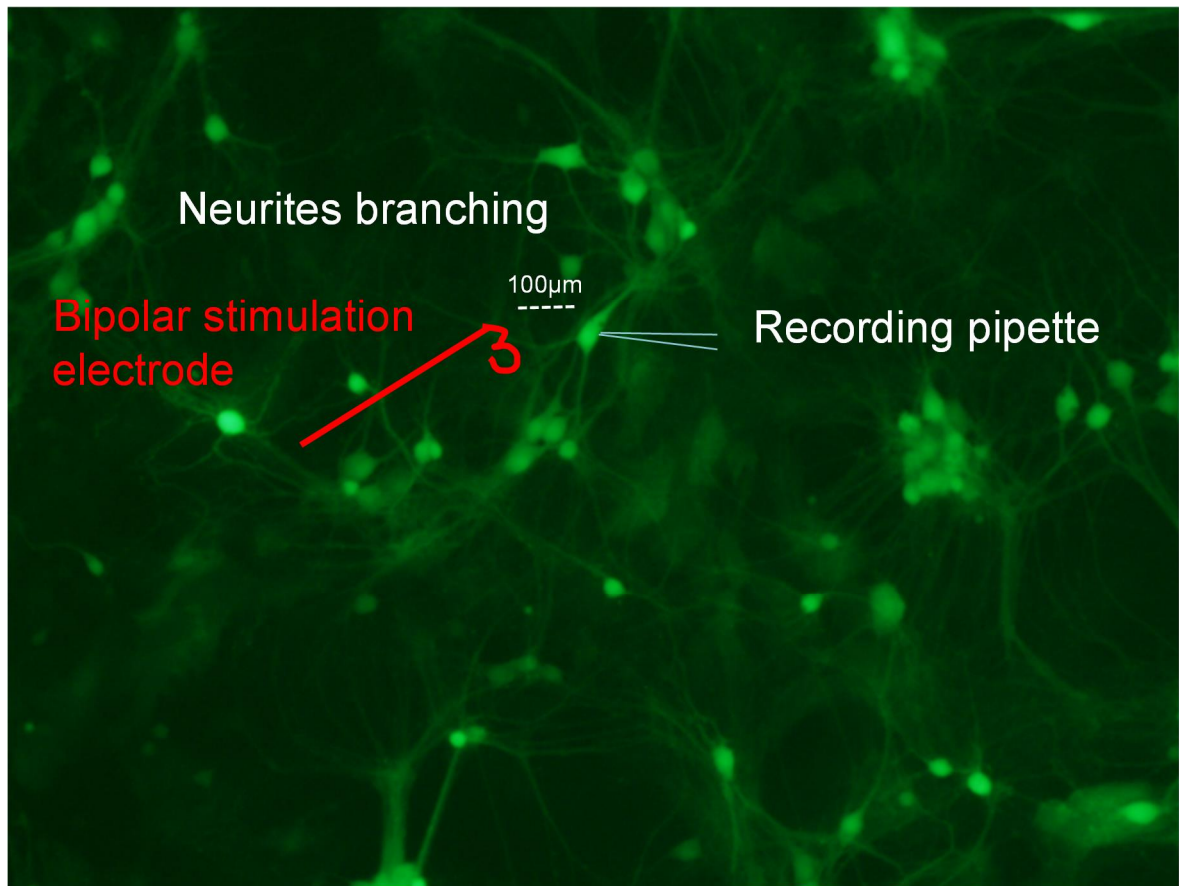


Figure 29. Experimental arrangement for electrical stimulation of cultured hippocampal neurons. Lentivirus infected neurons expressing GFP are shown in the image. Pyramidal neurons were selected for recording. Bipolar stimulation electrode was placed over neurites at 50-100 μm away from patched neurons.

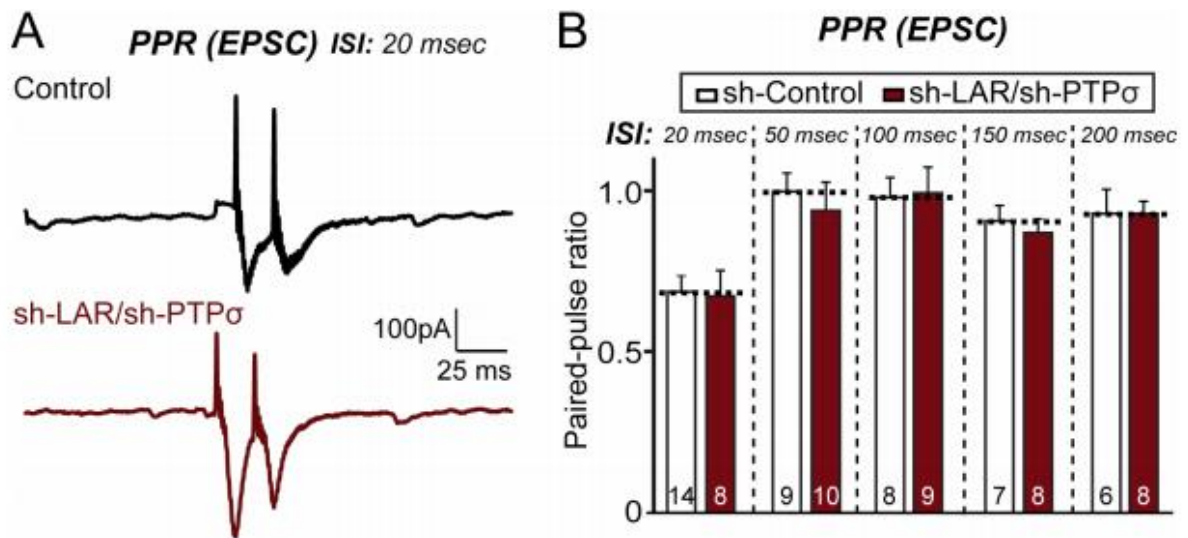


Figure 30. PTP is not essential for EPSC paired pulse ratio. EPSC paired pulse ratio was measured at 20, 50, 100, 150 and 200 ms inter stimulus interval (ISI) in control shRNA and sh-LAR/sh-PTP infected neurons. (A) Representative electrical traces. (B) Quantification of paired pulse ratio (EPSC2/EPSC1).

11. References

- Allen NJ, Bennett ML, Foo LC, Wang GX, Chakraborty C, Smith SJ, Barres BA (2012) Astrocyte glypicans 4 and 6 promote formation of excitatory synapses via GluA1 AMPA receptors. *Nature*. 486(7403):410-4.
- Boucard AA, Chubykin AA, Comoletti D, Taylor P, Sudhof TC (2005) A splice code for trans-synaptic cell adhesion mediated by binding of neuroligin 1 to alpha-and beta-neurexins. *Neuron*. 48:2296236.
- Brose N (2013) Why we need more synaptogenic cell-adhesion proteins. *Proc Natl Acad Sci U S A*. 110(10):3717-8.
- Chih, B., Engelman, H., and Scheiffele, P (2005) Control of excitatory and inhibitory synapse formation by neuroligins. *Science*. 307: 132461328
- Coles CH, Shen Y, Tenney AP, Siebold C, Sutton GC, Lu W, Gallagher JT, Jones EY, Flanagan JG, Aricescu AR (2011) Proteoglycan-specific molecular switch for RPTPsigma clustering and neuronal extension. *Science*. 332(6028):484-488.
- de Wit J, O'Sullivan ML, Savas JN, Condomitti G, Caccese MC, Vennekens KM, Yates JR 3rd, Ghosh A (2013) Unbiased discovery of glypican as a receptor for LRRTM4 in regulating excitatory synapse development. *Neuron*. 79(4):696-711.
- Desai CJ, Popova E, Zinn K (1994) A Drosophila receptor tyrosine phosphatase expressed in the embryonic CNS and larval optic lobes is a member of the set of proteins bearing the α HRP α carbohydrate epitope. *J Neurosci* 14:727267283
- Dieks JK, Gawinecka J, Asif AR, Vargas D, Gmitterova K, Streich JH, Dihazi H, Heinemann U, Zerr I (2013) Low-abundant cerebrospinal fluid proteome alterations in dementia with Lewy bodies. *J Alzheimers Dis*. 34:387-97.
- Gershon TR, Baker MW, Nitabach M, Wu P, Macagno ER (1998) Two receptor tyrosine phosphatases of the LAR family are expressed in the developing leech by specific central neurons as well as select peripheral neurons, muscles, and other cells. *J Neurosci* 18:29916 3002.

Gokce O, Südhof TC (2013) Membrane-tethered monomeric neurexin LNS-domain triggers synapse formation. *J Neurosci.* 33(36):14617-28.

Gray EG (1959) Axo-somatic and axo-dendritic synapses of the cerebral cortex: An electron microscope study. *J Anat* 93: 4206433.

Harata NC, Choi S, Pyle JL, Aravanis AM, Tsien RW (2006) Frequency-dependent kinetics and prevalence of kiss-and-run and reuse at hippocampal synapses studied with novel quenching methods. *Neuron* 49:2436256.

Herndon ME, Lander AD (1990) A diverse set of developmentally regulated proteoglycans is expressed in the rat central nervous system. *Neuron.* 6:949-61.

Hintsch G, Zurlinden A, Meskenaite V, Steuble M, Fink-Widmer K, Kinter J, Sonderegger P (2002) The calsyntenins--a family of postsynaptic membrane proteins with distinct neuronal expression patterns. *Mol Cell Neurosci.* 21:393-409.

Hoerndli FJ, Walser M, Fröhli Hoier E, de Quervain D, Papassotiropoulos A, Hajnal A. A conserved function of *C. elegans* CASY-1 calsyntenin in associative learning (2009) *PLoS One.* 4(3):e4880.

Ikeda DD, Duan Y, Matsuki M, Kunitomo H, Hutter H, Hedgecock EM, Iino Y (2008) CASY-1, an ortholog of calsyntenins/alcadeins, is essential for learning in *Caenorhabditis elegans*. *Proc Natl Acad Sci U S A.* 105:5260-5.

J.W. Um, J. Ko (2013) LAR-RPTPs: synaptic adhesion molecules that shape synapse development. *Trends Cell Biol.* 23:4656475

Johnson KG, Van Vactor D (2003) Receptor protein tyrosine phosphatases in nervous system development. *Physiol Rev.* 83(1):1-24.

Ko J, Soler-Llavina GJ, Fuccillo MV, Malenka RC, Südhof TC (2011) Neuroligins/LRRTMs prevent activity- and Ca²⁺/calmodulin-dependent synapse elimination in cultured neurons. *J Cell Biol.* 194(2):323-34.

Konecna A, Frischknecht R, Kinter J, Ludwig A, Steuble M, Meskenaite V, Indermühle M, Engel M, Cen C, Mateos JM, Streit P, Sonderegger P (2006) Calsyntenin-1 docks vesicular cargo to kinesin-1. *Mol Biol Cell.* 17:3651-63.

Lin X (2004) Functions of heparan sulfate proteoglycans in cell signaling during development. *Development*. 131(24):6009-21.

Litwack ED, Stipp CS, Kumbasar A, Lander AD (1994) Neuronal expression of glypican, a cell-surface glycosylphosphatidylinositol-anchored heparan sulfate proteoglycan, in the adult rat nervous system. *J Neurosci*. 14(6):3713-24.

Lu Z, Wang Y, Chen F, Tong H, Reddy MV, Luo L, Seshadrinathan S, Zhang L, Holthauzen LM, Craig AM, Ren G, Rudenko G (2014) Calsyntenin-3 molecular architecture and interaction with neurexin 1 . *J Biol Chem*. 289(50):34530-42.

Ludwig A, Blume J, Diep TM, Yuan J, Mateos JM, Leuthäuser K, Steuble M, Streit P, Sonderegger P (2009) Calsyntenins mediate TGN exit of APP in a kinesin-1-dependent manner. *Traffic*. 10:572-89.

Lüscher C, Isaac JT (2009) The synapse: center stage for many brain diseases. *J Physiol*. 587(Pt 4):727-9.

Maeda N, Ishii M, Nishimura K, Kamimura K (2011) Functions of chondroitin sulfate and heparan sulfate in the developing brain. *Neurochem Res*. 36(7):1228-40..

Missler M, Südhof TC, Biederer T (2012) Synaptic cell adhesion. *Cold Spring Harb Perspect Biol*. 2012 Apr 1; 4(4):1-18.

Ohno H, Kato S, Naito Y, Kunitomo H, Tomioka M, Iino Y (2014) Role of synaptic phosphatidylinositol 3-kinase in a behavioral learning response in *C. elegans*. *Science*. 345(6194):313-7.

Pettem KL, Yokomaku D, Luo L, Linhoff MW, Prasad T, Connor SA, Siddiqui TJ, Kawabe H, Chen F, Zhang L, Rudenko G, Wang YT, Brose N, Craig AM (2013) The specific - neurexin interactor calsyntenin-3 promotes excitatory and inhibitory synapse development. *Neuron*. 80:113-28.

Pettem KL1, Yokomaku D, Luo L, Linhoff MW, Prasad T, Connor SA, Siddiqui TJ, Kawabe H, Chen F, Zhang L, Rudenko G, Wang YT, Brose N, Craig AM (2013) The specific - neurexin interactor calsyntenin-3 promotes excitatory and inhibitory synapse development. *Neuron*. 80(1):113-28.

Ringman JM, Schulman H, Becker C, Jones T, Bai Y, Immermann F, Cole G, Sokolow S, Gylys K, Geschwind DH, Cummings JL, Wan HI (2012) Proteomic changes in cerebrospinal fluid of presymptomatic and affected persons carrying familial Alzheimer disease mutations. *Arch Neurol.* 69(1):96-104.

Scheiffele P, Fan J, Choih J, Fetter R, Serafini T (2000) Neuroligin expressed in nonneuronal cells triggers presynaptic development in contacting axons. *Cell* 101: 657-669.

Siddiqui TJ, Pancaroglu R, Kang Y, Rooyackers A, Craig AM (2010) LRRTMs and neuroligins bind neurexins with a differential code to cooperate in glutamate synapse development. *J Neurosci.* 30(22):7495-506.

Siddiqui TJ, Tari PK, Connor SA, Zhang P, Dobie FA, She K, Kawabe H, Wang YT, Brose N, Craig AM (2013) An LRRTM4-HSPG complex mediates excitatory synapse development on dentate gyrus granule cells. *Neuron.* 79(4):680-95.

Ster J, Steuble M, Orlando C, Diep TM, Akhmedov A, Raineteau O, Pernet V, Sonderegger P, Gerber U (2014) Calsyntenin-1 regulates targeting of dendritic NMDA receptors and dendritic spine maturation in CA1 hippocampal pyramidal cells during postnatal development. *J Neurosci.* 34:8716-27.

Steuble M, Diep TM, Schätzle P, Ludwig A, Tagaya M, Kunz B, Sonderegger P (2012) Calsyntenin-1 shelters APP from proteolytic processing during anterograde axonal transport. *Biol Open* 1:761-74.

Stipp CS, Litwack ED, Lander AD (1994) Cerebroglycan: an integral membrane heparan sulfate proteoglycan that is unique to the developing nervous system and expressed specifically during neuronal differentiation. *J Cell Biol.* 124(1-2):149-60.

Streuli M, Krueger NX, Ariniello PD, Tang M, Munro JM, Blattler WA, Adler DA, Disteché CM, Saito H (1992) Expression of the receptor-linked protein tyrosine phosphatase LAR: proteolytic cleavage and shedding of the CAM-like extracellular region. *EMBO J* 11:897-907.

Takahashi H & Craig AM (2013) Protein tyrosine phosphatases PTPdelta, PTPsigma, and LAR: presynaptic hubs for synapse organization. *Trends Neurosci.* 36(9):522-534.

Takahashi H, Arstikaitis P, Prasad T, Bartlett TE, Wang YT, Murphy TH, Craig AM (2011) Postsynaptic TrkC and presynaptic PTP function as a bidirectional excitatory synaptic organizing complex. *Neuron*. 69(2):287-303.

Takahashi H, Katayama K, Sohya K, Miyamoto H, Prasad T, Matsumoto Y, Ota M, Yasuda H, Tsumoto T, Aruga J, Craig AM (2012) Selective control of inhibitory synapse development by Slitrk3-PTP trans-synaptic interaction. *Nat Neurosci*. 15(3):389-98.

Tian SS, Tsoulfas P, Zinn K (1991) Three receptor-linked protein-tyrosine phosphatases are selectively expressed on central nervous system axons in the *Drosophila* embryo. *Cell* 67:675-680.

Uchida Y, Gomi F, Murayama S, Takahashi H (2013) Calsyntenin-3 C-terminal fragment accumulates in dystrophic neurites surrounding β plaques in tg2576 mouse and Alzheimer disease brains: its neurotoxic role in mediating dystrophic neurite formation. *Am. J. Pathol*. 182: 1718-1726.

Um JW, Pramanik G, Ko JS, Song MY, Lee D, Kim H, Park KS, Südhof TC, Tabuchi K, Ko J (2014) Calsyntenins function as synaptogenic adhesion molecules in concert with neuroligins. *Cell Rep*. 6:1096-109.

Vagnoni A, Perkinton MS, Gray EH, Francis PT, Noble W, Miller CC (2012) Calsyntenin-1 mediates axonal transport of the amyloid precursor protein and regulates A β production. *Hum Mol Genet*. 21(13):2845-54.

Vogt L, Schimpf SP, Meskenaite V, Frischknecht R, Kinter J, Leone DP, Ziegler U, Sonderegger P (2001) Calsyntenin-1, a proteolytically processed postsynaptic membrane protein with a cytoplasmic calcium-binding domain. *Mol Cell Neurosci*. 17:151-66.

Woo J, Kwon SK, Choi S, Kim S, Lee JR, Dunah AW, Sheng M, Kim E (2009) Trans-synaptic adhesion between NGL-3 and LAR regulates the formation of excitatory synapses. *Nat Neurosci*. 12(4):428-37.

Yan H, Grossman A, Wang H, D'Eustachio P, Mossie K, Musacchio JM, Silvennoinen O, Schlessinger J (1993) A novel receptor tyrosine phosphatase-sigma that is highly expressed in the nervous system. *J Biol Chem* 268:24880-24886

Yim YS, Kwon Y, Nam J, Yoon HI, Lee K, Kim DG, Kim E, Kim CH, Ko J (2013) Slitrks control excitatory and inhibitory synapse formation with LAR receptor protein tyrosine phosphatases. *Proc Natl Acad Sci U S A*. 110(10):4057-62.

Yin GN, Lee HW, Cho JY, Suk K (2009) Neuronal pentraxin receptor in cerebrospinal fluid as a potential biomarker for neurodegenerative diseases. *Brain Res*. 1265:158-70.

Yoshida T, Yasumura M, Uemura T, Lee SJ, Ra M, Taguchi R, Iwakura Y, Mishina M (2011) IL-1 receptor accessory protein-like 1 associated with mental retardation and autism mediates synapse formation by trans-synaptic interaction with protein tyrosine phosphatase . *J Neurosci*. 31(38):13485-99.

Zhang C, Atasoy D, Arac, D, Yang X, Fucillo MV, Robison AJ, Ko J, Brunger AT, Sudhof TC (2010) Neurexins physically and functionally interact with GABA(A)receptors. *Neuron*66:4036416.

12. Abbreviations

A

ACSF Artificial Cerebro-Spinal Fluid

B

BSA Bovine serum albumin

BME Basal Medium Eagle

C

CST-1 Calsyntnin-1

CST-2 Calsyntnin-2

CST-3 Calsyntnin-3

cAMP Cyclic adenosine monophosphate

cDNA Complementary DNA

COS-7 African green monkey cell line

CNQX 6-cyano-7-nitroquinoxaline-2,3-dione

CaCl₂ Calcium Chloride

CST-TKD CST triple knockdown

CST-SKD CST single knockdown

D

DMEM Dulbecco's Modified Eagle Medium

DMSO Dimethylsulfoxid

DNA	Deoxyribonucleic acid
Dnase	Desoxyribonuclease
DNQX	6,7-dinitroquinoxaline-2,3-dione
DIV	Day of <i>in vitro</i>

E

EPSC	Excitatory postsynaptic current
EGFP	Enhanced Green Fluorescent Protein
E.Coli	Escherichia coli
EDTA	Ethylenediaminetetraacetic acid
EGTA	Ethylene Glycol Tetraacetic Acid
E15.5	Embryonic day 15.5

F

FBS	Fetal bovine serum
-----	--------------------

G

GABA	-Amino butyric acid
GAPDH	Glyceraldehyde 3-phosphate dehydrogenase
GAD	Glutamate decarboxylase
GST	Glutathione S-transferase
GPC	Glypican
GFP	Green Fluorescent Protein

G Giga ohm

H

HBSS Hank's balanced salt solution

HEPES 4-(2-hydroxyethyl)-1-piperazineethanesulfonic acid

Hz Hertz

HSPG Heparan sulfate proteoglycan

HS Heparan sulfate

HEK Human Embryonic Kidney 293 cells

HEK293T Human Embryonic Kidney 293 cells

HA Hemagglutinin

I

IPSC Inhibitory postsynaptic current

IF Immunofluorescence

IgG Immunoglobulin G

IN Interneurons

IP Immunoprecipitation

K

kDa kilo Dalton

KCl Potassium chloride

L

LRRTM	Leucin-rich repeats transmembrane
LRRTM-DKD	Leucin-rich repeats transmembrane double knockdown
LNS	laminin/Nrx/sex hormone-binding globulin
LAR-RPTPs	Leukocyte common antigen-related receptor protein tyrosine phosphatases
LAR	leucocyte common antigen

M

MAP2	Microtubule associated protein 2
mRNA	Messenger RNA
mIPSCs	miniature inhibitory postsynaptic currents
mEPSCs	miniature excitatory postsynaptic currents
MgSO ₄	Magnesium sulfate
M	Mega ohm
Mg-ATP	Adenosine 5 -triphosphate magnesium salt
MPBS	Modified phosphate buffer saline

N

NIH	National Institute of Health
Na-GTP	Guanosine 5 -triphosphate sodium salt hydrate
NaCl	Sodium Chloride
NL1	NL 1

NL2	NL 2
Nrx-TKD	Nrxs triple knockdown
P	
PPR	paired pulse ratio
PAGE	Polyacrylamide Gel Electrophoresis
PIPES	Piperazine-N,Nø-bis(ethanesulfonic acid); 1,4-piperazinediethanesulfonic acid
PBS	Phosphate Buffered Saline
PCR	Polymerase Chain Reaction
PFA	Parafolmaldehyde
PEI	polyethyleneimine
PTP	Protein tyrosine phosphatase sigma
PTP	Protein tyrosine phosphatase delta
P12-20	post natal day 12-20
P0-P3	post natal day 0-3
PEST	Penicillin/Streptomycin
Q	
qRT-PCR	Quantitative Real - Time Polymerase chain reaction
R	
rpm	Rotations per minute

RNA	Ribonucleic acid
RT	Room temperature
RT-PCR	Reverse Transcriptase Polymerase Chain Reaction

S

SDS	Sodium Dodecyl Sulfate
SEM	Standard Error Mean
SliTrks	Slit- and Trk-like proteins
sh-Nrx1/2/3	sh-Nrx1/sh-Nrx2/sh-Nrx3

T

TAE	Tris-Acetate-EDTA
TBS	Tris Buffered Saline
TEMED	Tetramethylethylenediamine
Tris	Tris(hydroxymethyl)-aminomethane
TTX	Tetrodotoxin

13. Curriculum Vitae

Name: Gopal Pramanik
Current Position: PhD scholar
Address: South Sibpur, Debnibas, Namkhana,
24PGS(S), West Bengal, India, 743357



Telephone: +81-7013248899

Email Address gopal.stemcell@gmail.com
gopal@shinshu-u.ac.jp
gopal@nips.ac.jp

Institute address: Department of Molecular and Cellular Physiology,
Shinshu University School of Medicine, 3-1-1
Asahi, Matsumoto, 390-8621 Japan

University:

2012-now: PhD student in the school of life sciences, National Institute for Physiological Sciences, The Graduate University of Advanced Studies (Sokendai) Okazaki, Japan (Prof. Yumiko Yoshimura) and Molecular and Cellular Physiology, Shinshu School of Medicine (Prof. Dr. K. Tabuchi).

2007-2011: Research scholar in the Institute of Physiology at the Faculty of Medicine of the Otto-von-Guericke-University Magdeburg (Prof. Dr. V. Leßmann).

2005-2007: Research scholar, School of Biological Sciences, Nanyang Technological University, Singapore (Asst. Prof. Dr. Koh Cheng Gee).

2002-2004: Master of Technology in biotechnology and biochemical engineering, Department of Biotechnology, Indian Institute of Technology (IIT) Kharagpur, Kharagpur, India (Prof. Dr. S.H. Dey). Grade: õgoodö.
Title of master thesis: Expression of recombinant human FGF8b in plants by transformation using *Agrobacterium rhizogenes* and *Agrobacterium tumefaciens* mediated vacuum infiltration, and raising polyclonal anti-FGF8b antibodies in rabbit. Grade: övery goodö.

1998-2002: Bachelor of Pharmaceutical Technology, Department of Pharmaceutical Technology, Jadavpur University, WB, India. Grade: õgoodö.
Title of bachelor thesis: Surveys of anthelmintic drugs

Fields of experience and interest: Neurobiology, electrophysiology, patch clamp recording, imaging, live-cell imaging, cell biology, molecular biology

Work and Research Experiences:

Laboratory skills:

Neurobiology- Electrophysiology, Imaging, primary neuron culture, slice physiology, in utero electroporation

- É Culture of neuronal cells at low density
- É Calcium phosphate transfection of neurons with DNA plasmids
- É Imaging of GFP labeled protein inside cells
- É FM labeling of synaptic vesicles
- É Live-cell imaging of transfected neurons
- É Whole cell patch clamp recordings of cultured neurons
- É Cell attached patch clamp recordings of cultured neurons
- É Combined live-cell imaging and patch clamp recordings
- É BDNF secretion assay
- É Assay of fusion pore opening of BDNF-EGFP containing vesicle using bromphenol blue

- É Preparation of handmade local perfusion.
- É In utero electroporation in cortex and hippocampus
- É Infection of cultured neurons with lentivirus

Cell and tissue culture- culture of CHO cells, Cos7 cells, HeLa, NIH3T3, isolation and culture of embryonic fibroblast from mouse embryos, culture of mouse embryonic stem cells (CCE, D3) and stem cell differentiation by embryoid body formation to neuron, culture of human embryonic stem cells on feeder cells and matrix gel, transfection of stem cells and cell lines.

DNA/RNA/protein works- plasmid DNA purification, RNA purification, protein purification, PCR, Western blotting

Staining and Microscopy- immuno-cell staining of stem cells and cell lines, confocal microscopy, eppifluorescence microscopy and live cell imaging

Softwares learnt- Patch Master, Minianalysis software (synptosoft), Clampex, Clampfit, Metavue, Microsoft Excel, Corel Draw, and LSM-510.

Bioinformatics- BLAST homology search, multiple sequence alignment, primer designing (Primer-3), Clustal X.

Other: Preliminary experience in AAV production and injection of AAV in mouse brain by stereotaxic injection.

Major projects:

2012-now: Research scholar in the Division of Cerebral Structure, National Institute for Physiological Sciences, The Graduate University of Advanced Studies (Sokendai) Okazaki, Japan.

Project- Role of CAMs in synaptic transmission and synaptic plasticity in culture neurons and acute brain slices.

Aim of this project is to study role of specific CAMs such as CSTs, LAR-RPTP proteins in synapse formation and synaptic transmissions. I am using several LAR-RPTP lentiviral shRNA, mutant, and rescue constructs to investigate specific function of given CAMs: PTPs,

PTPd and LAR in culture rat hippocampal neurons. I am recording different presynaptic and postsynaptic responses by whole cell patch clamp recordings.

For acute brain slice whole cell patch clamp recording I am performing in utero electroporation in embryonic brains. The specific brain regions expressing shRNA, mutant, rescue proteins are used for electrophysiological recordings. Currently I am transfecting shRNA of CSTs in mouse by in utero electroporation and am using transfected mouse for patch clamp recording of mIPSCs, mEPSCs, PPR-EPSC/IPSC, etc.

2007-2011: Junior scientist at the Institute of Physiology, Faculty of Medicine, Otto-von-Guericke-University Magdeburg, Germany.

Project- Patterns of electrical activity supporting fusion pore opening and release of BDNF from BDNF-containing vesicles in dendrites of hippocampal neurons.

Current project deals with the patterns of electrical activity in hippocampal neurons which are necessary and sufficient to observe BDNF secretion at synapses

I used calcium phosphate transfection method to transfect BDNF-EGFP plasmid DNA in hippocampal neurons. I combined live-cell imaging of BDNF- GFP containing vesicles in cultured hippocampal neurons, and whole cell patch clamp recording and cell attached tight seal voltage clamp recording of transfected neurons, to correlate electrical activity of the hippocampal neurons with release events of BDNF- GFP containing vesicles.

During my work, so far, I established different assays to visualize fusion pore events and compound release of BDNF-GFP from single secretory granules, and whole cell recording and cell attached tight seal voltage clamp recording conditions which allow for prolonged recording of electrical signals without interfering with release events. My results indicate that short bursts of action potentials (approx. 20 APs) can induce efficient fusion pore opening of BDNF-GFP vesicles specifically in distal dendrites of hippocampal neurons, whereas compound release is dependent on ongoing electrical activity within a certain interval after fusion pore opening. I also observed spontaneous action potential (17APs) induced BDNF secretion in culture neuron in cell specific manner. Interestingly opening of cell to whole cell patch clamp configuration can also induce BDNF secretion that is dependent on extra cellular calcium. The cytoplasmic

dilution and extra cellular calcium dependent BDNF secretion on opening of cell to whole cell configuration lead study of action potential induced BDNF secretion is very challenging: Especially correlating physiological number of action potential required to induce BDNF secretion in hippocampal neuron that is important for spike timing dependent plasticity (STDP) paradigm of synaptic plasticity, learning and memory.

I implemented cell attached tight seal voltage clamp recording in BDNF secretion assay to investigate action potential induced BDNF secretion without disturbing cytoplasm of the neuron. The cell attached tight seal voltage clamp recording is advantageous over whole cell patch clamp recording and perforated patch clamp recording especially for peptide secretion assay: The cell attached patch does not disturb cytoplasmic environment of cell, easy to implement and less time consuming. I am successful in induction of BDNF secretion by stimulating BDNF-EGFP over-expressed cultured hippocampal neuron in cell attached tight seal voltage clamp recording mode. The most challenging part of project is to devise suitable stimulation condition which could differentiate role of action potential and depolarization in induction of BDNF secretion.

It would be interesting to study action potential-induced and depolarization-induced fusion pore opening and compound secretion of BDNF containing vesicles using finest tools such as BROMOPHENOL BLUE and BDNF-superecliptic-Phluorin in separate experiments. So far synaptic vesicles exocytosis cycle has been extensively studied by different scientists; but action potential (physiological numbers of APs) mediated peptide secretion and peptide vesicles exocytosis and endocytosis is not widely investigated.

2005-2007: Research scholar, School of Biological Sciences, Nanyang Technological University, Singapore.

Project- The study of Rho-GTPases mediated cell-signaling in embryonic stem cell.

Aim was to study the effect of Rho GTPases on stem cell cytoskeleton, morphology, proliferation and differentiation. I have done preliminary screening for the expression of RhoGTPases and their effectors in mouse embryonic stem cells using RT-PCR, western blotting and immunofluorescent staining. I found that three of the most commonly studied

RhoGTPases (Cdc42, Rac1, and RhoA) and their effectors were expressed in mouse embryonic stem cells. There were no apparent morphology changes found in mouse embryonic stem cells (CCE) on over expression of different RhoGTPases. The higher level of mDia1, an effector of RhoA, was expressed in mouse embryonic stem cell (CCE) than differentiated cells and embryoid bodies (EBs).

2002-2004: Master of Technology in biotechnology and biochemical engineering, Department of Biotechnology, Indian Institute of Technology Kharagpur, Kharagpur, India.

Project- Expression of recombinant human FGF8b in plants by transformation using *Agrobacterium rhizogenes* and *Agrobacterium tumefaciens* mediated vacuum infiltration; and raising polyclonal anti-FGF8b antibodies in rabbit.

Human proteins are not properly fold and modified in bacterial expression systems. Aim of the project was to express FGF8b in tobacco and spinach plants, characterization of expressed proteins. Anti-FGF8b antibodies was produced in rabbit for the characterization expressed FGF8b in plants.

Award for academic proficiency: Emami Award Winner from Indian Pharmaceutical association (IPA), State of West Bengal branch as a highest GATE (graduate aptitude test in engineering) scorer with all India rank 72 in 2002.

Symposium speaker:

Gopal Pramanik (2014) Synapse formation and function regulated by structural alteration of Nrxs. **S2: S2-1** Synapses, Neural Circuits, and Neuropsychiatric Disorder. KSBMB (Korean Society for Biochemistry and Molecular Biology) Annual Meeting. May 14, Seoul, South Korea.

13. Scientific Publications

13.1. Posters:

Pramanik G, Ko J, Shigemoto R, Tabuchi K (2012). CST regulated synaptic transmission in inhibitory synapses in somatosensory cortex. JSPS Symposium "Mechanisms of synaptic transmission", Doshisha University, December 6-7, Doshisha, Japan.

Edelmann E, **Pramanik G**, Brigadski T, Leßmann, V (2011). The role of BDNF secretion in Spike Timing-Dependent Plasticity. Proc. 9th Göttingen Meeting of the German Neuroscience Society, March 23-26, Göttingen, Germany.

Pramanik G, Brigadski T, Leßmann, V (2009). Comparison of the secretion of BDNF from hippocampal cultures induced by high-potassium depolarisation and backpropagating action potentials. Proc. 8th Göttingen Meeting of the German Neuroscience Society, March 25-29, Göttingen, Germany.

Pramanik G, Brigadski T, Leßmann, V (2009). Fusion kinetics of BDNF containing vesicles in response to burst discharges of action potentials in hippocampal neurons. CBBS Evaluation Symposium, Magdeburg, Germany.

13.2. Papers:

Um JW, **Pramanik G**, Ko JS, Song MY, Lee D, Kim H, Park KS, Südhof TC, Tabuchi K and Ko J (2014) CSTs Function as Synaptogenic Adhesion Molecules in Concert with Nrxs. Cell Rep 6(6):1096-1109

Tabuchi K, Hang W, Asgar NF, **Pramanik G**. (2014) Synapse maturation and autism: learning from NL model mice. Nihon Shinkei Seishin Yakurigaku Zasshi. 34(1):1-4. (Japanese).

Ji Seung Ko, **Gopal Pramanik**, Ji Won Um, Ji Seon Shim, Kee Hun Kim, GugYoung Chung, Minhye Kim, Ho Min Kim, Joris de Wit, Kang-Sik Park, Katsuhiko Tabuchi, Jaewon Ko (2015). PTP acts as a presynaptic receptor for glypican-4/LRRTM4 complex and is essential for excitatory synaptic transmission. PNAS (Ji Seung Ko, Gopal Pramanik and Ji Won Um contributed equally in this work).